Bollettino di Geofisica Teorica ed Applicata Vol. 58, n. 4, pp. 313-342; December 2017
DOI 10.4430/bgta0216

Seismogenic zonation as a branch of the logic tree for the new Italian seismic hazard map - MPS16: a preliminary outline

M. Santulin[1], A. Tamaro[2], A. Rebez[2], D. Slejko[2], F. Sani[3], L. Martelli[4], M. Bonini[5], G. Corti[5], M.E. Poli[6], A. Zanferrari[6], A. Marchesini[6], M. Busetti[2], M. Dal Cin[2, 7], D. Spallarossa[8], S. Barani[8], D. Scafidi[8], G. Barreca[9] and C. Monaco[9]

[1] *Istituto Nazionale di Geofisica e Vulcanologia, Sezione di Milano, c/o OGS, Trieste, Italy*
[2] *Istituto Nazionale di Oceanografia e di Geofisica Sperimentale - OGS, Trieste, Italy*
[3] *Dip. di Scienze della Terra, Università di Firenze, Italy*
[4] *Servizio Geologico, Sismico e dei Suoli, Regione Emilia-Romagna, Bologna, Italy*
[5] *Istituto di Geoscienze e Georisorse, Consiglio Nazionale delle Ricerche, Firenze, Italy*
[6] *Dip. di Scienze AgroAlimentari, Ambientali e Animali, Università di Udine, Italy*
[7] *Dip. di Matematica e Geoscienze, Università di Trieste, Italy*
[8] *Dip. di Scienze della Terra dell'Ambiente e della Vita, Università di Genova, Italy*
[9] *Dip. di Scienze Biologiche, Geologiche e Ambientali, Università di Catania, Italy*

(Received: August 10, 2017; accepted December 15, 2017)

ABSTRACT The zonation presented in this study has been developed with the aim of applying it as a branch of the logic tree that will be used for the new Italian seismic hazard map, presently in preparation according to the approach of seismotectonic probabilism. With respect to the zonation used for the present official seismic hazard map of Italy, the zonation proposed here considers narrower sources and is based on new and updated seismological data. In particular, some new seismogenic zones are proposed here, introducing areas that were not considered seismogenic until now (e.g., the narrow sources characterised by the presence of transform faults which are almost normal to the trend of the northern Apennines). The preliminary seismic hazard estimates produced with this new zonation aim to identify possible problems that the zonation introduces in the seismicity characterization of the seismogenic zones. As the present seismic hazard assessment was computed by considering a different attenuation model with respect to the one applied for the previous national seismic hazard maps, a re-elaboration of the most recent map referring to Italy has been developed: the comparison of the two maps is a good indicator of the areas where additional seismological investigation is needed to support the zonation presented here. In particular, some zones are not adequately documented with regard to seismicity and a different computation of the seismicity rates is suggested.

1. Introduction

The importance of seismogenic zonation has been widely demonstrated through sensitivity analysis (e.g., Rebez and Slejko, 2000; Barani *et al.*, 2007) as one of the most influential parameters in a seismic hazard assessment using the seismotectonic probabilism approach. The

© 2017 – OGS

definition of the seismogenic sources is generally based on evidence coming from tectonics and seismicity. In the Italian context, it is generally hard to find a direct relation between the two pieces of information since, in practice, it is anything but simple to identify tectonic structures with documented seismic activity [see e.g., both national (Slejko *et al.*, 1998; Meletti *et al.*, 2008) and regional (Slejko *et al.*, 2011) seismogenic models proposed in the literature]. Usually, geology identifies tectonic structures that were, and maybe still are, active. Frequently, seismicity depicts earthquakes scattered in broad areas, where many faults exist. In addition, the geometry of the faults at depth is unknown and cannot be inferred from surface geology. For these reasons, a different way to establish a link between geology and seismicity is needed: the definition of a general kinematic framework (Meletti *et al.*, 2000; Schmid and Slejko, 2009) is one way to do it. Based on this kinematic framework, seismotectonic regions, i.e., tectonically homogeneous areas with similar seismic behaviour, are identified, and these regions lead to mapping seismogenic zones that collect one fault, or alternatively a homogeneous fault population, with associated earthquakes.

Even forgetting that in a previous version of the Italian seismic law [technical enclosure no. 1 of Ordinanza PCM 3274 (2003)] a revision of the national seismic hazard map was expected every five years, it is common practice worldwide to update the national seismic hazard maps when new science justifies it. In the case of Italy, more than 10 years have passed since the elaboration which the present national building code is based on, and a national project is now in progress aimed at introducing all new data and science into the new Italian seismic hazard map (hereafter cited as MPS16).

The zonation presented here has been developed with the aim of applying it as a branch of the logic tree that will be used for the computation of MPS16, where additional types of information (fault characteristics, geodetic data) and approaches (smoothed seismicity) will be considered as well. This new hazard map is expected to replace the present official one [named MPS04 (Stucchi *et al.*, 2011)], which is the reference for the present Italian building code, and will be calculated, as was the previous one, according to the approach of seismotectonic probabilism, originally proposed by Cornell (1968). This approach is based on two hypotheses:

1) earthquake occurrence intervals follow an exponential distribution (i.e., earthquakes constitute a Poisson process);
2) magnitude is distributed exponentially according to the Gutenberg – Richter (GR) relation.

A third hypothesis is that seismicity is considered uniformly distributed inside each seismic source (this condition is, actually, already considered in the definition of the seismic source itself).

The Cornell (1968) method needs the following input data: the seismic source geometry, the earthquake potential (which is defined in terms of average number of earthquakes per magnitude class, and maximum magnitude), and one or more ground motion attenuation models. In the present study, the seismic sources have been modelled as wide seismogenic zones (SZs), in agreement with the previous zonations [ZS4 by Meletti *et al.* (2000) and ZS9 by Meletti *et al.* (2008)] used for the Italian seismic hazard maps (Slejko *et al.*, 1998; Stucchi *et al.*, 2011).

Uncertainty quantification (McGuire, 1977; McGuire and Shedlock, 1981; Toro *et al.*, 1997) represents a crucial point in probabilistic seismic hazard analysis (PSHA), and both the aleatory variability (randomness of natural phenomena) and the epistemic uncertainty (limited quantity of

data and insufficient knowledge about the earthquake process) are taken into account respectively with proper standard deviations of the parameters used and the use of a suitable logic tree (Kulkarni *et al.*, 1984; Coppersmith and Youngs, 1986).

The hazard computation presented here aims to identify possible limits in the use of the present zonation for hazard purposes in order to, in the very near future, fix those limits.

Motivating the development of a new national seismic hazard map was the availability of new data and studies that highlighted the possibility of a better definition of the potentially SZs of the Apennines and of the Po Plain with respect to the ZS9 (Meletti *et al.*, 2008) used for the calculation of the MPS04 map (Stucchi *et al.*, 2011). This new zonation (called zonation A1 hereafter) has been developed through a detailed analysis of the existing national zonations performed by the common work of four groups of local experts in seismotectonics (Fig. 1).

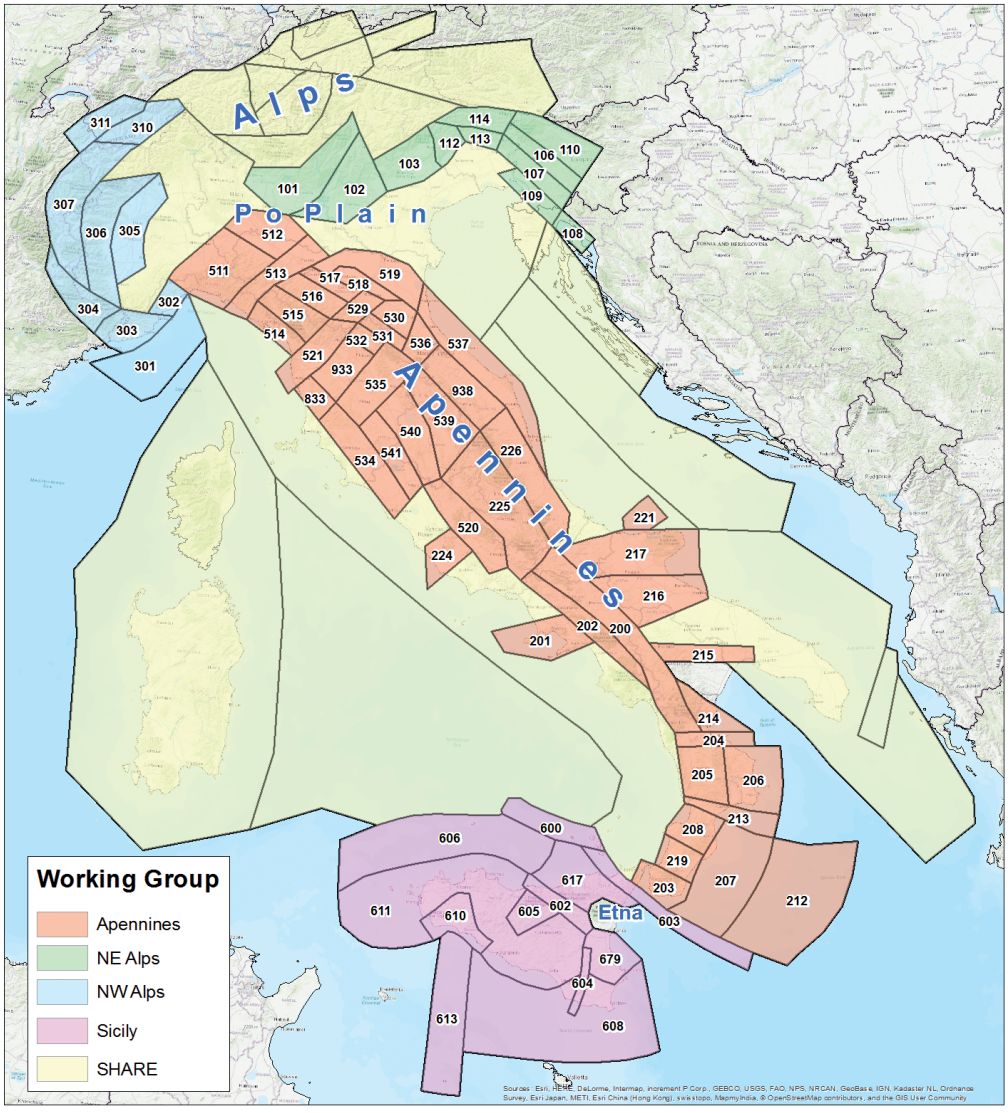

Fig. 1 - The A1 zonation. Different colours identify the SZs proposed by the four teams of experts contributing to this model. The SZs taken from the SHARE project are also highlighted.

In the new zonation, the seismotectonic conditions are considered homogeneous within each SZ whose geometry has been defined, taking into account available information on:

- epicentral distribution of earthquakes from the new historical earthquake catalogue CPTI15 (Rovida *et al.*, 2016) and regional bulletins of instrumental seismicity (Scafidi *et al.*, 2015);
- observed (Rovida *et al.*, 2016) and/or estimated (DISS Working Group, 2015; Wells and Coppersmith, 1994) M_{max};
- focal mechanisms [from the European-Mediterranean Regional Centroid Moment Tensor (RCMT) catalogue (Pondrelli *et al.*, 2011)];
- hypocentral depth (Pondrelli *et al.*, 2011; DISS Working Group, 2015; ISIDe Working Group, 2015);
- geometry, type and kinematics of potentially active or recent (Quaternary) structures identified on the basis of morphological and structural data and integrated with the sources from the database of the Italian seismogenic sources DISS 3.2.0 (DISS Working Group, 2015) and the available literature;
- regional strain rate fields derived from seismic and GPS data (e.g., Delacou *et al.*, 2008; Barani *et al.*, 2010).

2. The logic tree for seismic hazard assessment

As it is not the aim of this paper to produce a new PSHA but to propose a new zonation and identify its possible limits when applied for hazard purposes, a simple logic tree with only six branches (Fig. 2) has been considered in the present study: three branches account for the epistemic uncertainty in the seismicity model and two branches are related to alternative values of the maximum magnitude (M_{max}). Conversely, the suite of ground motion prediction equations (GMPEs) to be used for the final national map has not yet been selected. Consequently, a single attenuation model has been applied in the present preliminary PSHA as a demonstration.

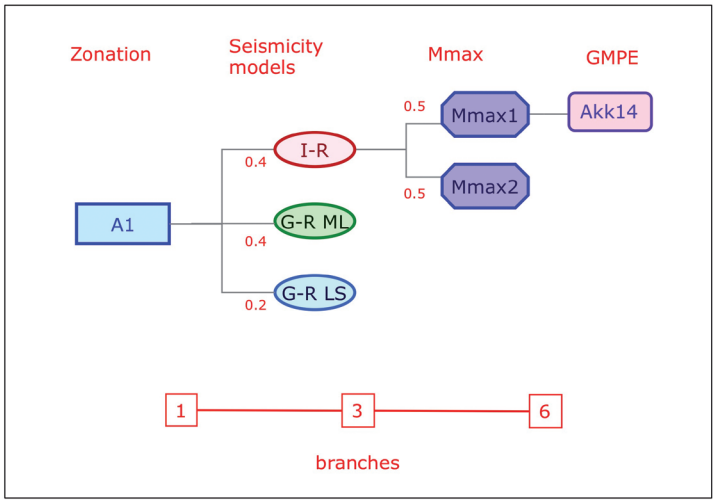

Fig. 2 - The logic tree used for the preliminary seismic hazard assessment with the A1 zonation. It consists of three seismicity models (see the text for the details) and two estimates for M_{max} (see the text for details). The numbers indicate the weights associated with each branch (see the text for details).

Concerning the node relative to the seismicity model, one branch accounts for individual rates (I-R; i.e., the non-cumulative number of earthquakes in the magnitude bins, without their interpolation with the GR fit), while the remaining two use different approaches to compute the values of the GR coefficients (*a*- and *b*-values): one uses the Least Squares (LS) approach (GR-LS) and one adopts the Maximum Likelihood (ML) method (GR-ML) according to the formulation proposed by Weichert (1980). The application to seismicity rate computation of the LS method, although often used, is not formally correct, since magnitude is not error free, cumulative event counts are not independent, and the error distribution of the number of earthquake occurrences does not follow a Gaussian distribution. Conversely, the ML method is formally correct and has been widely applied: Weichert (1980) proposed a general routine that also accounts for different completeness periods for the various magnitude classes of the earthquakes in the catalogue. For these reasons, a weight of 0.4 has been applied to the I-R branch and to the ML one, while only 0.2 has been assigned to the LS branch (Fig. 1).

The two values for M_{max} have been identified on the basis of the maximum observed or estimated earthquake in each SZ, increasing those estimates by the related standard deviation and additionally by 0.3. A weight of 0.5 has been applied to each M_{max} branch, as no specific reason exists to prefer one to the other.

3. The new zonation

In defining the zone boundaries, particular attention has been paid to the general kinematic context, to the regional seismotectonic setting, and to the seismic history, in order to avoid excessive extrapolation of local features, which could lead to an underestimation of the hazard produced by more active local structures and to an overestimation of the hazard related to less active sources.

For each SZ, a failure mechanism has been proposed (Pondrelli *et al.*, 2011; DISS Working Group, 2015):

- geometry of the failure plane (strike and dip);
- fault kinematics (normal, reverse, strike-slip, or mixed);
- hypothesized hypocentral depth (range).

For some SZs, more failure mechanisms have been considered possible; in such cases, various estimates of the percentage of seismicity have been assigned (depending on the information available). The seismogenic zonation proposed and applied for the computation of the European seismic hazard map, developed within the framework of the SHARE project (Woessner *et al.*, 2015), has also been taken into account to model SZs at the borders of the national territory, and outside it.

The new zonation A1 is generally more detailed when compared to ZS9 (Meletti *et al.*, 2008), and has taken the zonation ZS4 (Meletti *et al.*, 2000) deeply into consideration. For some of the new SZs, the difference between them and those of the ZS9 zonation has been found to be negligible in terms of geographical boundaries and seismotectonic characteristics: these SZs, slightly modified with respect to the ZS9 zonation, are highlighted in bold in Table 1. Summarizing, the A1 zonation consists of 77 SZs, 6 of which mimic the ZS9 geometry, while ZS9 and ZS4 count 36 and 80 SZs, respectively.

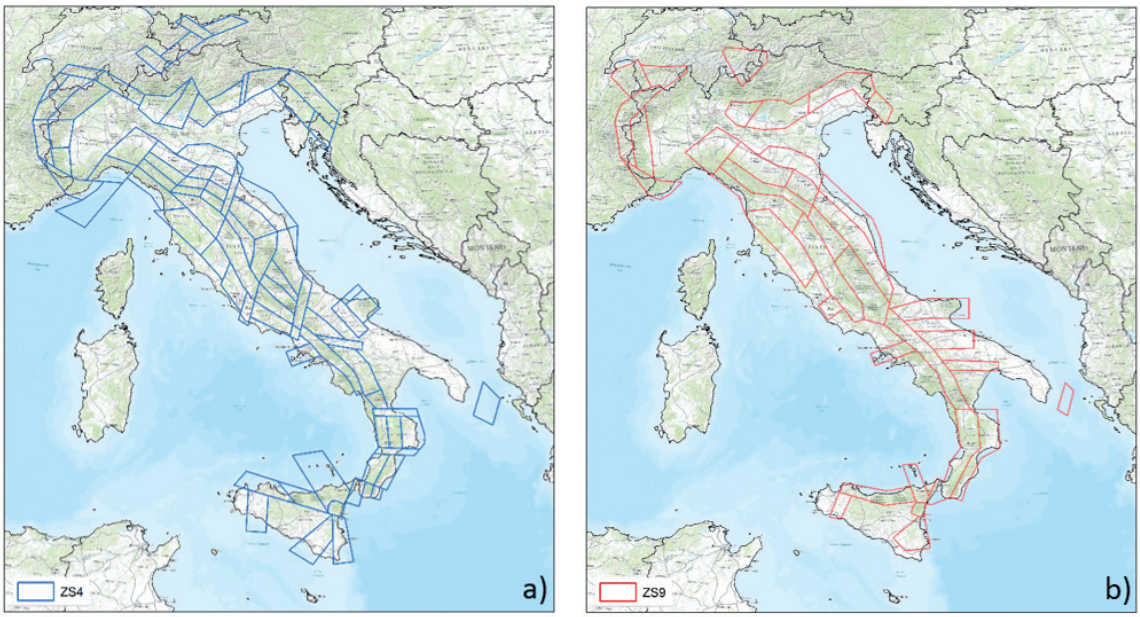

Fig. 3 - The seismogenic zonations existing in the literature for Italy that have been considered in the present study: a) ZS4; b) ZS9.

The main novelties of the proposed zonation are:

- a subdivision of some very large SZs of ZS9 which, in the authors' opinion, include seismogenic structures with different geometry and failure mechanisms;
- the introduction of new SZs, including areas not considered seismogenic until now [e.g., the narrow SZs characterised by the presence of transform faults which are almost normal to the trend of the northern Apennines: a full explanation about the new SZs is given in Martelli *et al*. (2017a, 2017b, 2017c)].

By comparing the new zonation A1 (Fig. 1) with the previous ones (Fig. 3), it can be noted that the new SZs are more similar in dimension to those of the ZS4 zonation (Fig. 3a) than to those of ZS9 (Fig. 3b). The limited dimensions of the SZs in ZS4 came about because of the need to satisfy the condition of tectonic homogeneity requested by the Cornell (1968) approach. Conversely, ZS9 was designed with fewer, but wider zones than ZS4, considering that the spread space distribution of small earthquakes, due to limits in earthquake location, invalidate the possibility of constraining strong and weak events in narrow SZs. Moreover, it is well known that the computation of the seismicity rates is poorly constrained for small SZs where the events are few. These aspects have been considered in designing zonation A1 by looking for an acceptable balance between seismotectonic homogeneity and number of events in the SZs (see more details in the description of the seismicity rates). The small SZs present in the A1 zonation are fully supported by specific tectonic characteristics; nevertheless, the present analysis also aims at identifying problematic situations for seismicity characterization. In such cases, a modification of the SZ geometry would be taken into account only in cases where seismicity characterization would not be feasible.

It is important to note that the Etna area has not been included in the present study, because the definition of the seismic source responsible for the seismicity related to the volcano is the subject of a separate study within the framework of the MPS16 project.

4. Seismic hazard

Seismic hazard has been computed for the national territory on the basis of the new seismogenic zonation A1 and the revised and updated seismological data, using OpenQuake software (Pagani *et al.*, 2014).

The new version of the Italian Parametric Catalogue CPTI15 (Rovida *et al.*, 2016) was the only seismological source: it represents significant innovation with respect to the previous Italian earthquake catalogues because:

- the time coverage has been extended from 2006 to the end of 2014;
- existing data in the previous national catalogue CPTI11 (Rovida *et al.*, 2011) have been updated and new instrumental data have been added;
- the energy thresholds have been lowered to intensity 5, equated to magnitude 4.0, instead of the 5-6 and 4.5, respectively, of the previous version;

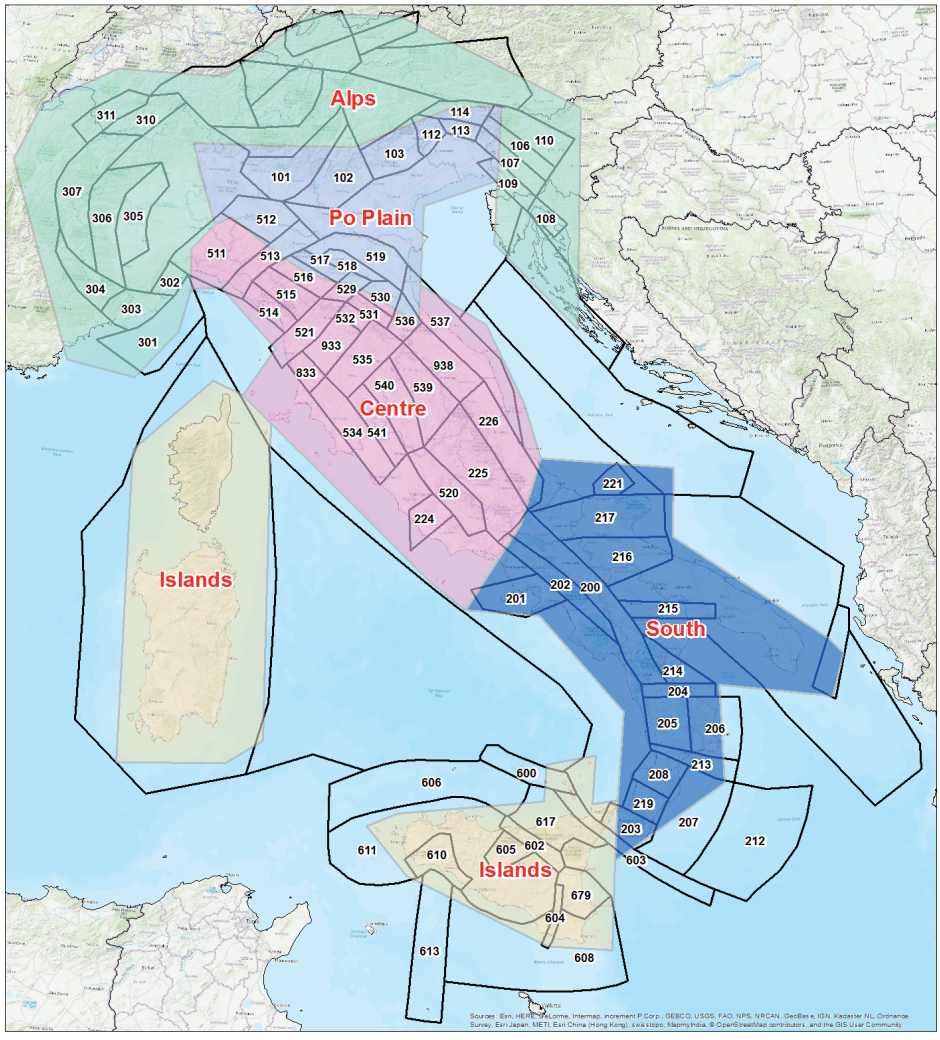

Fig. 4 - The A1 zonation (boxes with black perimeter) and macro areas (coloured polygons) identifying homogeneous regions for the assessment of completeness.

- the determination of the hypocentral parameters from macroseismic data has been based on a new calibration of the Boxer software (Gasperini *et al.*, 1999);
- the instrumental magnitudes derive from new data sets and new scaling laws, available in the documentation of the CPTI15 catalogue (Rovida *et al.*, 2016).

The catalogue covers the entire Italian territory together with some neighbouring areas and seas. It collects 4584 earthquakes in the time period 1000-2014, 4390 of them have a focal depth lower than 60 km and suitably to represent the seismicity of the SZs. Earthquake magnitude is expressed in terms of moment magnitude (M_W) for all earthquakes in the catalogue, and the related uncertainty is provided.

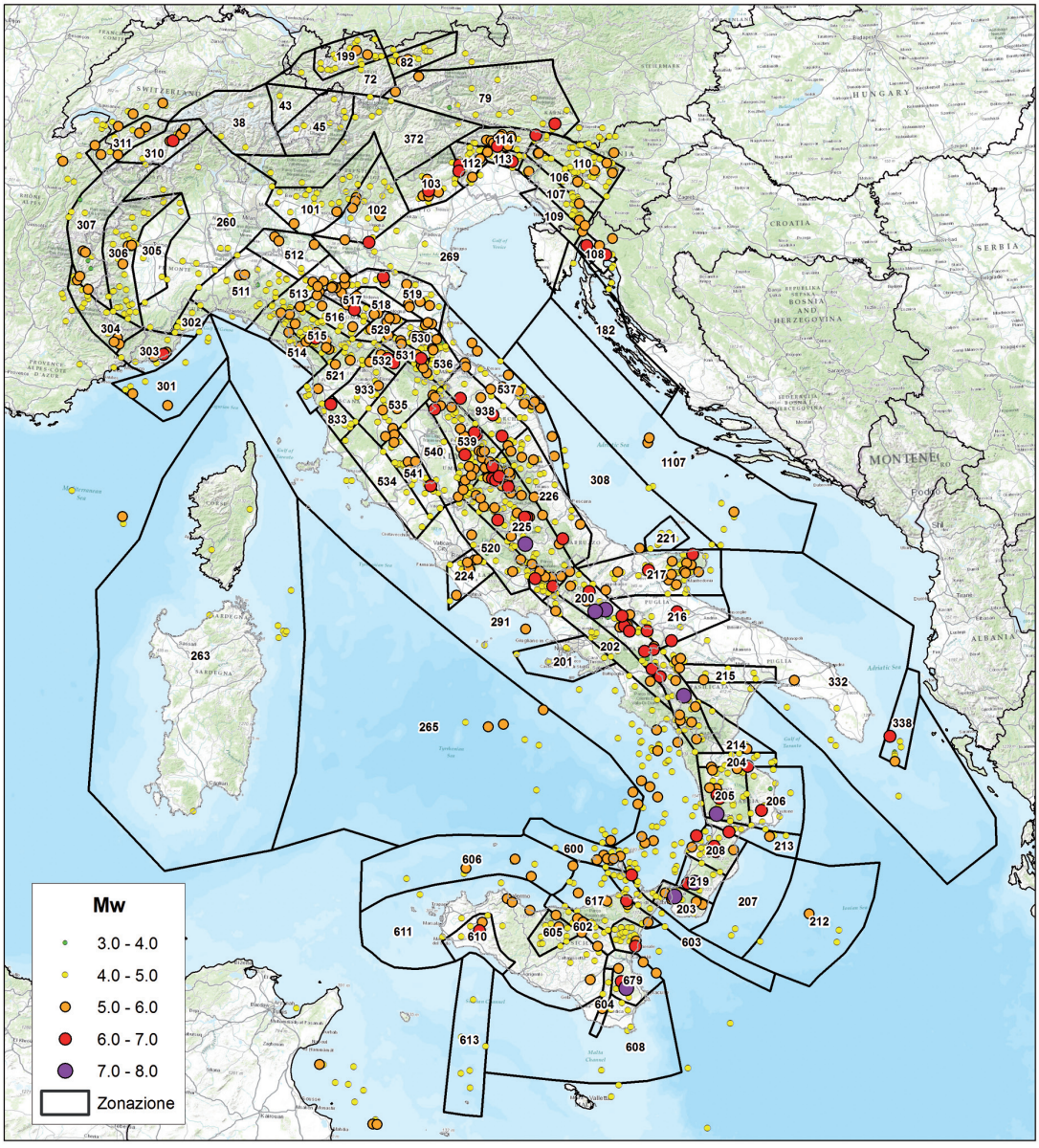

Fig. 5 - The A1 zonation and the epicentres of the earthquakes of the CPTI15 catalogue (after the declustering process).

Because the CPTI15 catalogue includes foreshocks and aftershocks, it has been necessary to remove the dependent events in order to fulfill the Poisson assumption underlying the seismicity process. This operation was achieved by declustering the catalogue by the application of a space and time window (Gardner and Knopoff, 1974), based on a proper table, and a related map for the space application of the table itself, provided by the CPTI15 compilers, together with similar table and map (Fig. 4) to be used for the identification of the completeness periods of the various magnitude classes. A total of 3323 independent earthquakes remained in the catalogue after the declustering process, out of the 4390 original events (Fig. 5).

In the present PSHA, zonation A1 has taken full advantage of the potential of the software OpenQuake (Pagani *et al.*, 2014): for each SZ, one or more rupture mechanisms have been considered as possible (different or not, depending on the information available, see Fig. 6 and Table 1); in such cases, various percentages of seismicity have been assigned to the two or more mechanisms. To cover the whole national territory, the values of the rupture mechanisms selected by SHARE (Woessner *et al.*, 2015) have also been adopted in the present elaboration (Table 2) for the SZs taken from the SHARE project.

Table 1 - Summary of the rupture mechanisms for zonation A1 based on geological considerations and calibrated on literature data (Pondrelli *et al.*, 2011; DISS Working Group, 2015). Bold numbers identify the SZs that are only slightly modified with respect to the ZS9 zonation. Legenda: usd = upper source depth, lsd = lower source depth, npw = nodal plane weight, hd = hypocentre depth, hdw = hypocentre depth weight.

No.	Name	usd	lsd	strike1	strike2	dip1	dip2	rake1	rake2	npw1	npw2	hd	hdw
101	Lombardian Prealps	5	15	225	225	35	35	90	90	0.5	0.5	8	1
102	Lessini- Verona Plain	5	20	140	140	90	90	180	180	0.5	0.5	12	1
103	Venetian Prealps	5	15	240	240	40	40	90	90	0.5	0.5	10	1
106	Idrija - Bovec	10	20	135	135	90	90	180	180	0.5	0.5	15	1
107	Cividale-Postojna	10	20	135	135	90	90	180	-100	0.8	0.2	15	1
108	Rijeka	4	15	315	315	65	65	170	170	0.5	0.5	10	1
109	Trieste	4	15	315	315	65	65	170	170	0.5	0.5	10	1
110	Western Slovenia	10	20	125	125	90	90	180	180	0.5	0.5	15	1
112	Central-Western Carnic Prealps	5	15	240	240	40	40	90	75	0.5	0.5	9	1
113	Central Friuli	6	10	290	270	35	35	100	110	0.5	0.5	8	1
114	Carnia	10	15	150	115	90	90	180	180	0.5	0.5	12	1
200	**Southern Apennines**	**1**	**20**	**315**	**160**	**50**	**70**	**-90**	**-90**	**0.5**	**0.5**	**10**	**1**
201	Napoli-Salerno	1	10	225	225	70	80	-90	-90	0.5	0.5	5	1
202	Caserta-Avellino-Battipaglia	1	20	315	315	60	80	-90	-90	0.5	0.5	9	1
203	Reggio -Messina	1	20	20	20	20	40	-90	-90	0.5	0.5	8	1
204	Calabria Transverse Castrovillari-Rossano	1	20	270	270	70	80	-90	-90	0.5	0.5	9	1
205	Inner Calabria north	1	20	180	180	60	70	-90	-90	0.5	0.5	9	1
206	Eastern Calabrian arc	1	20	180	180	20	40	90	90	0.5	0.5	8	1
207	Internal Ionian Sea	10	50	180	250	20	20	90	90	0.5	0.5	30	1
208	Inner Calabria central part	1	20	20	20	35	45	-90	-90	0.5	0.5	8	1

Table 1 - continued.

No.	Name	usd	lsd	strike1	strike2	dip1	dip2	rake1	rake2	npw1	npw2	hd	hdw
212	External Ionian Sea	1	20	180	250	20	20	90	90	0.5	0.5	10	1
213	Calabria transverse north	1	20	90	90	80	90	0	180	0.5	0.5	12	1
214	Amendolara	1	20	315	315	10	10	90	90	0.5	0.5	10	1
215	**Potenza-Matera-Taranto**	**10**	**25**	**270**	**270**	**70**	**90**	**0**	**180**	**0.5**	**0.5**	**18**	**1**
216	Barletta	1	20	250	250	70	70	-90	-90	0.5	0.5	8	1
217	Gargano zone modified	3	25	270	270	70	90	0	180	0.5	0.5	14	1
219	Inner Calabria south	1	20	20	20	20	40	-90	-90	0.5	0.5	7	1
221	Tremiti	1	20	225	225	30	50	90	90	0.5	0.5	10	1
224	**Alban Hills**	**1**	**20**	**225**	**225**	**60**	**90**	**-90**	**0**	**0.6**	**0.4**	**10**	**1**
225	**Abruzzo Apennines**	**1**	**20**	**225**	**225**	**50**	**70**	**-90**	**-90**	**0.5**	**0.5**	**10**	**1**
226	Abruzzo	10	35	135	135	30	30	90	90	0.5	0.5	23	1
301	Ligurian Sea	1.1	12.5	180	90	45	45	90	90	0.5	0.5	5	1
302	Liguria	1.4	8.3	180	90	90	90	0	0	0.5	0.5	6	1
303	Ligurian Alps	1.4	9.5	180	90	90	90	0	0	0.5	0.5	6	1
304	Maritime Alps	2	8.7	180	90	45	90	-90	0	0.5	0.5	5	1
305	Western Po Plain	14.2	44.9	180	90	45	45	90	90	0.5	0.5	34	1
306	External Branch of Western Alps	6.1	13.8	180	90	45	45	90	-90	0.5	0.5	11	1
307	Internal Branch of Western Alps	1	8.8	180	90	45	45	-90	-90	0.5	0.5	5	1
310	Pennine Alps	1.6	8.4	180	90	45	45	-90	-90	0.5	0.5	5	1
311	Swiss Prealps	1.4	10.8	180	90	90	90	0	0	0.5	0.5	6	1
511	Liguria	1	20	225	225	90	90	0	180	0.5	0.5	8	1
512	Emilia Folds	5	30	90	180	45	90	90	0	0.8	0.2	18	1
513	Taro-Enza	5	30	225	90	90	53	0	90	0.8	0.2	18	1
514	NW Coastal Sector	5	15	135	315	65	65	-90	-90	0.5	0.5	8	1
515	Garfagnana	1	20	315	135	65	65	-90	-90	0.6	0.4	5,15	0.8 0.2
516	Emilia Apennines	1	20	270	90	65	30	-90	90	0.8	0.2	8	1
517	Emilia Margin	10	30	90	90	45	60	90	90	0.5	0.5	20	1
518	Nonantola-Budrio	15	35	90	120	15	30	90	90	0.5	0.5	23	1
519	Ferrara Folds	5	15	90	120	45	45	90	90	0.5	0.5	10	1
520	Latium Apennines	1	20	135	135	60	70	-90	-90	0.5	0.5	10	1
521	Pistoia-Pisa	1	20	225	135	90	65	0	-90	0.8	0.2	9	1
529	Reno-Setta	1	35	210	90	90	53	0	90	0.8	0.2	6,25	0.8 0.2
530	Romagna Margin	5	35	90	90	30	45	90	90	0.5	0.5	6	1
531	Romagna Apennines	3	10	315	120	65	30	-90	90	0.8	0.2	6	1
532	Mugello	1	20	120	300	65	65	-90	-90	0.6	0.4	6	1
534	Tusco-Latium Littoral	1	20	135	135	65	65	-90	-90	0.5	0.5	6	1
535	Casentino-Valdarno-Siena	1	20	225	135	90	65	0	-90	0.8	0.2	6	1

Table 1 - continued.

No.	Name	usd	lsd	strike1	strike2	dip1	dip2	rake1	rake2	npw1	npw2	hd	hdw
536	Savio-Marecchia	1	25	210	120	90	30	0	90	0.8	0.2	6,20	0.8 0.2
537	**Adriatic Folds**	**5**	**15**	**135**	**135**	**45**	**45**	**90**	**90**	**0.5**	**0.5**	**6**	**1**
539	**Umbria**	**1**	**20**	**135**	**330**	**53**	**53**	**-90**	**-90**	**0.6**	**0.4**	**6**	**1**
540	Trasimeno	1	20	160	160	65	65	-90	-90	0.5	0.5	6	1
541	Amiata-Bolsena	1	20	160	160	65	65	-90	-90	0.5	0.5	6	1
600	Sisifo-Alicudi (South-eastern Tyrrhenian)	0	35	290	290	85	85	180	180	0.5	0.5	6	1
602	Cefalù-Etna	0	30	300	300	85	85	180	180	0.5	0.5	6	1
603	Tindari -Letojanni (Ionian fault)	5	15	310	310	85	85	180	180	0.5	0.5	6	1
604	Scicli	20	30	20	20	90	90	0	0	0.5	0.5	6	1
605	Central Sicily	0	30	225	225	45	45	90	90	0.5	0.5	6	1
606	Solunto High	0	20	225	225	60	60	90	90	0.5	0.5	6	1
608	Sicily Channel Rift Zone	0	20	100	100	90	90	180	180	0.5	0.5	6	1
610	Belice Valley	0	30	260	260	45	45	90	90	0.5	0.5	6	1
611	Siciliy background	0	30	225	225	45	45	90	90	0.5	0.5	6	1
613	N-S Belt Sicily Channel	0	20	0	0	90	90	180	180	0.5	0.5	6	1
617	Nebrodi	0	35	45	45	45	45	-90	-90	0.5	0.5	6	1
679	North-eastern edge of the Hyblean Plateau and Catania Plain	0	30	105	250	90	45	180	90	0.5	0.5	6	1
833	Val di Fine	1	20	160	160	60	70	-90	-90	0.5	0.5	6	1
933	Florence-Volterra	1	20	135	225	65	90	-90	0	0.8	0.2	6	1
938	Marche north	10	35	135	135	30	30	90	90	0.5	0.5	6	1

Individual seismicity rates have been computed for each SZ, using the data of the declustered CPTI15 catalogue and considering the completeness periods provided by the catalogue compilers (no information about the recent seismicity has been considered for the seismic characterization of the SZs; the regional catalogues have been used only for the definition of the SZ geometry). The seismicity rates have been computed for bins of 0.3 magnitude units. Then, seismicity rates at a 0.1 sampling rate have been recomputed from the GR fit (Aki, 1965; Utsu, 1965, 1966) of the cumulative number of events. As said before, two among the different methodologies for assessing the coefficients (*a*- and *b*-values) of the GR relation available in literature have been applied in this work: the LS and the ML methods (GR-LS red line and GR-ML blue line, respectively, in Fig. 7). This latter regression has been done according to the Weichert (1980) method, and Fig. 7 and Table 3 show the results obtained. It can be seen that the *b*-value for some SZs is outside the range that is usually considered acceptable (e.g., 0.3 for SZ 206, 0.4 for SZ 679, 1.55 for SZ 603, 1.61 for SZ 540, 1.95 for SZ 938): in some cases (e.g., SZs 540 and 603), this is due to the small number of magnitude classes documented in the GR relation, and in others more investigation is needed to identify the reason for the strange GR behaviour.

Table 2 - Summary of the rupture mechanisms of the SHARE SZs.

No.	Name	strike1	dip1	RakeSS	RakeNorm	RakeRev	WeightSS	WeightNorm	WeightRev	hd1
38	CHAS098	0	90	0	-90	90	0.7	0.25	0.05	10
43	CHAS099	0	90	0	-90	90	0.7	0.25	0.05	10
45	CHAS100	0	90	0	-90	90	0.7	0.25	0.05	10
72	ATAS133	0	90	0	-90	90	0.7	0.25	0.05	10
79	ATAS164	280	75	0	-90	90	0.2	0.6	0.2	8
82	ATAS165	58	67	0		90	0.7		0.3	10
182	HRAS215	317	37	0	-90	90	0.3	0.05	0.65	13
199	ATAS166	0	90	0	-90	90	0.7	0.25	0.05	9
260	ITAS284	310	37	0	-90	90	0.7	0.25	0.05	9
263	ITAS306	0	90	0	-90	90	0.33	0.33	0.34	10
265	ITAS309	0	90	0	-90	90	0.3	0.2	0.5	10
269	ITAS287	305	41	0	-90	90	0.3	0.05	0.65	9
291	ITAS296	302	73	0	-90	90	0.2	0.3	0.5	13
308	ITAS301	284	67	0	-90	90	0.3	0.05	0.65	13
332	ITAS312	320	30	0	-90	90	0.35	0.15	0.5	13
338	ALAS314	0	90	0	-90	90	0.4	0.1	0.5	11
372	ITAS327	0	90	0	-90	90	0.7	0.25	0.05	9
1107	HRAS188	302	44	0	-90	90	0.4	0.1	0.5	13

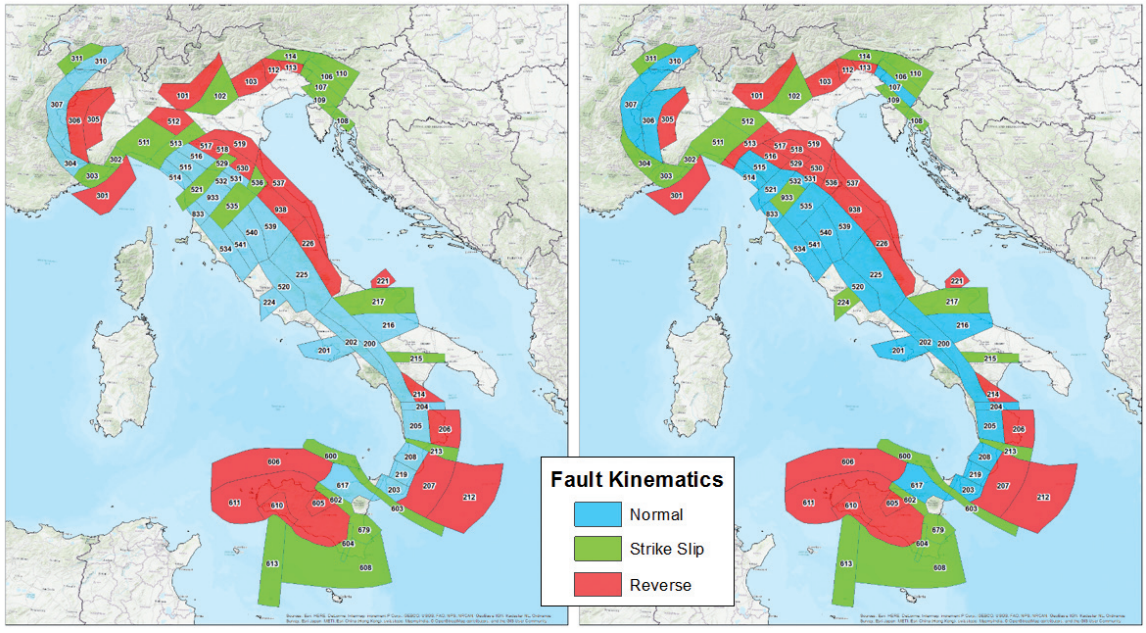

Fig. 6 - The two models of fault kinematics used in the hazard computation. The two different mechanisms that characterize a few SZs are illustrated in the two panels with different colours: blue = normal, green = strike-slip, red = reverse.

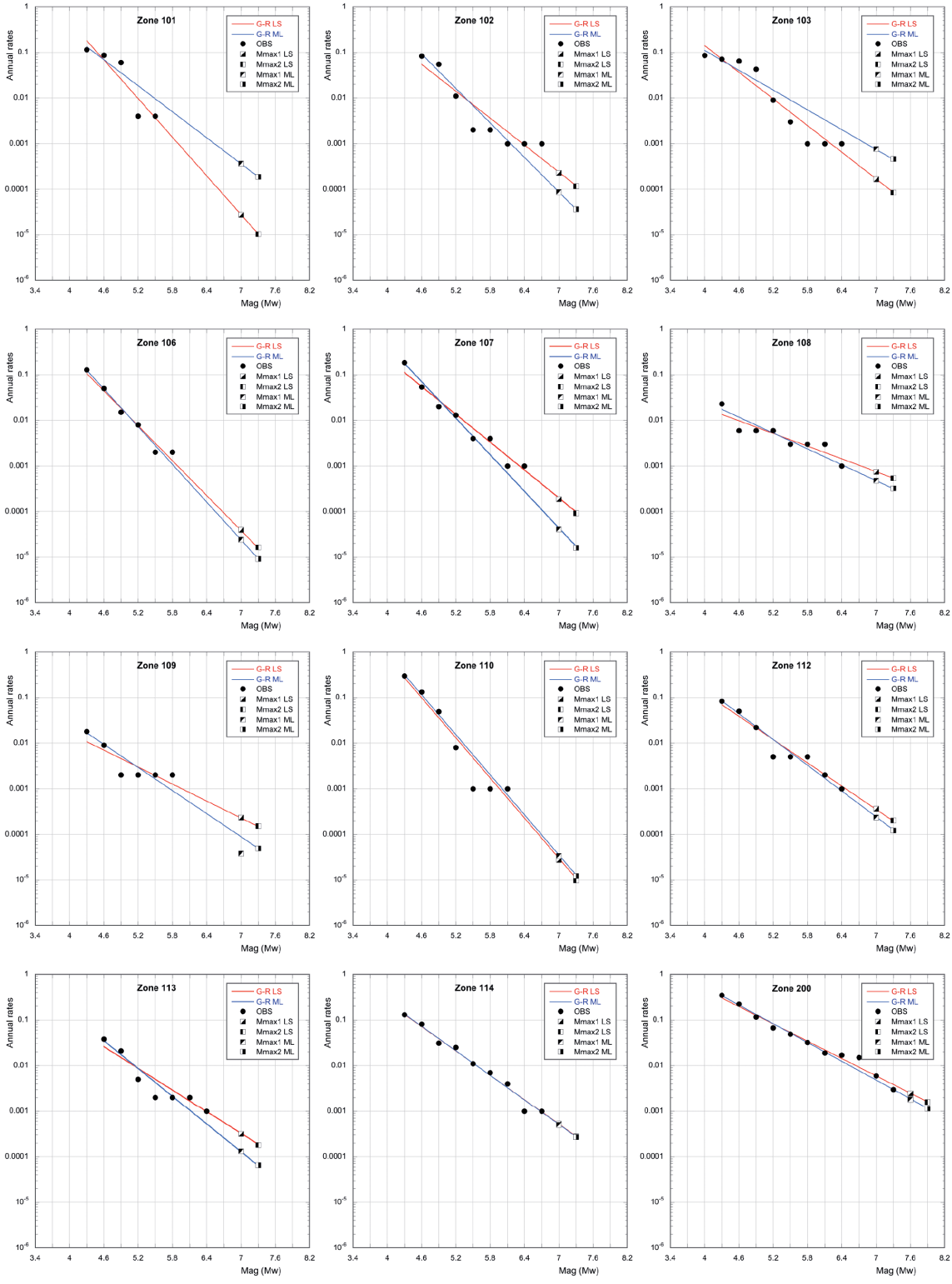

Fig. 7 - G-R curves referring to the A1 zonation, obtained by the Least Squares (red line, GR-LS) and the Maximum Likelihood (blue line, GR-ML) approaches. Black dots represent the observed individual seismicity rates. The different squares distinguish the M_{max1} and M_{max2} rates.

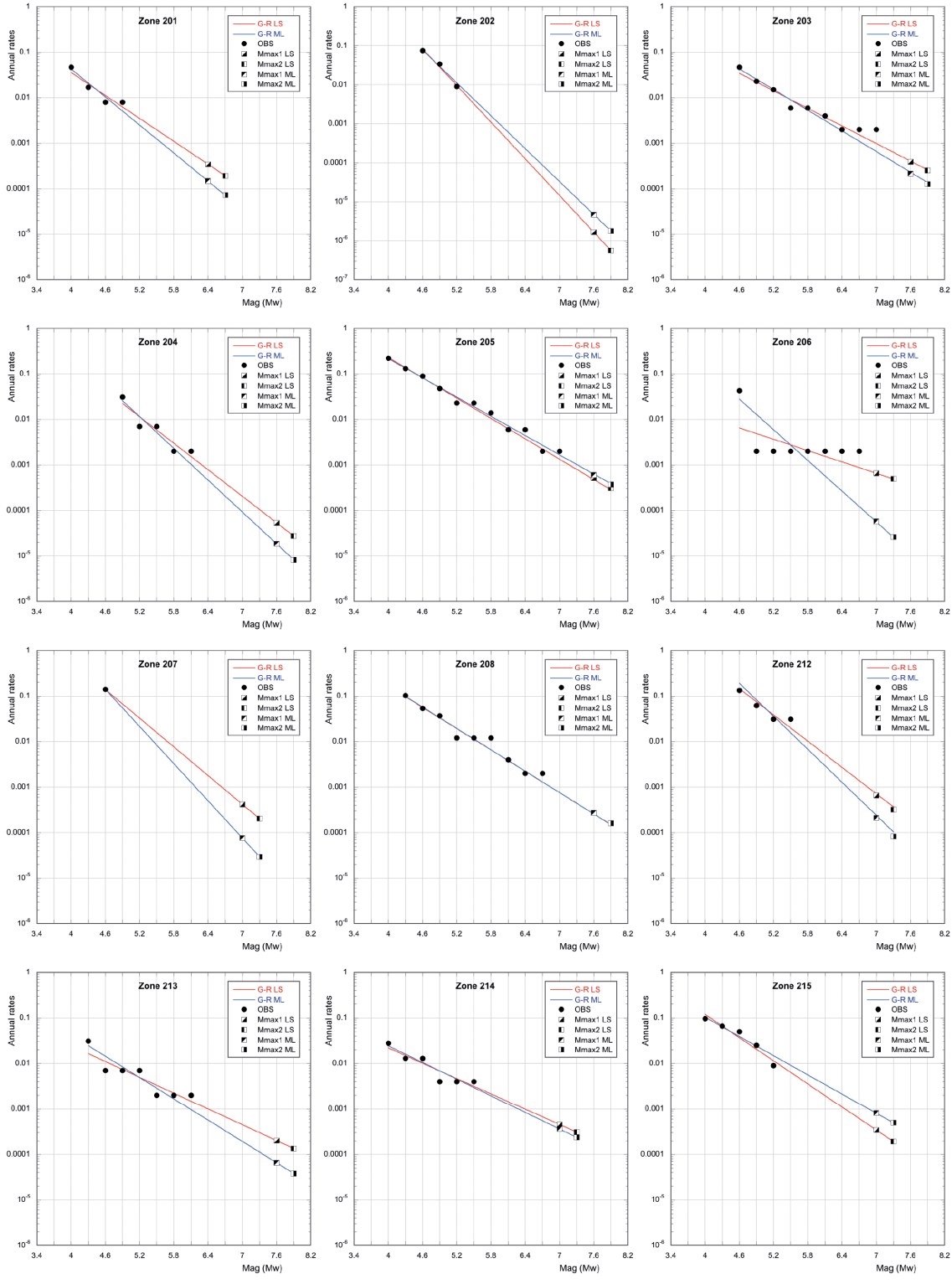

Fig. 7 - continued.

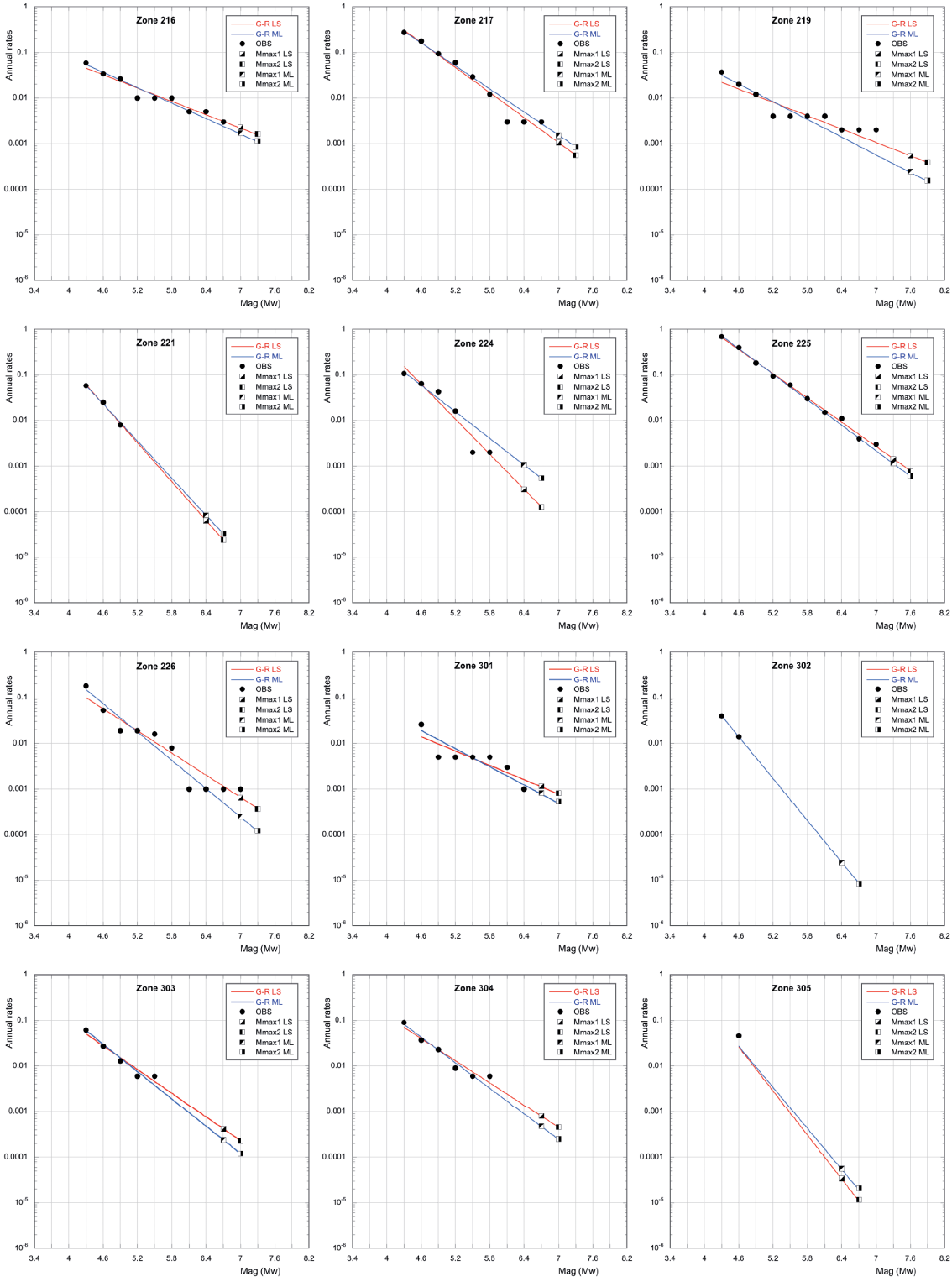

Fig. 7 - continued.

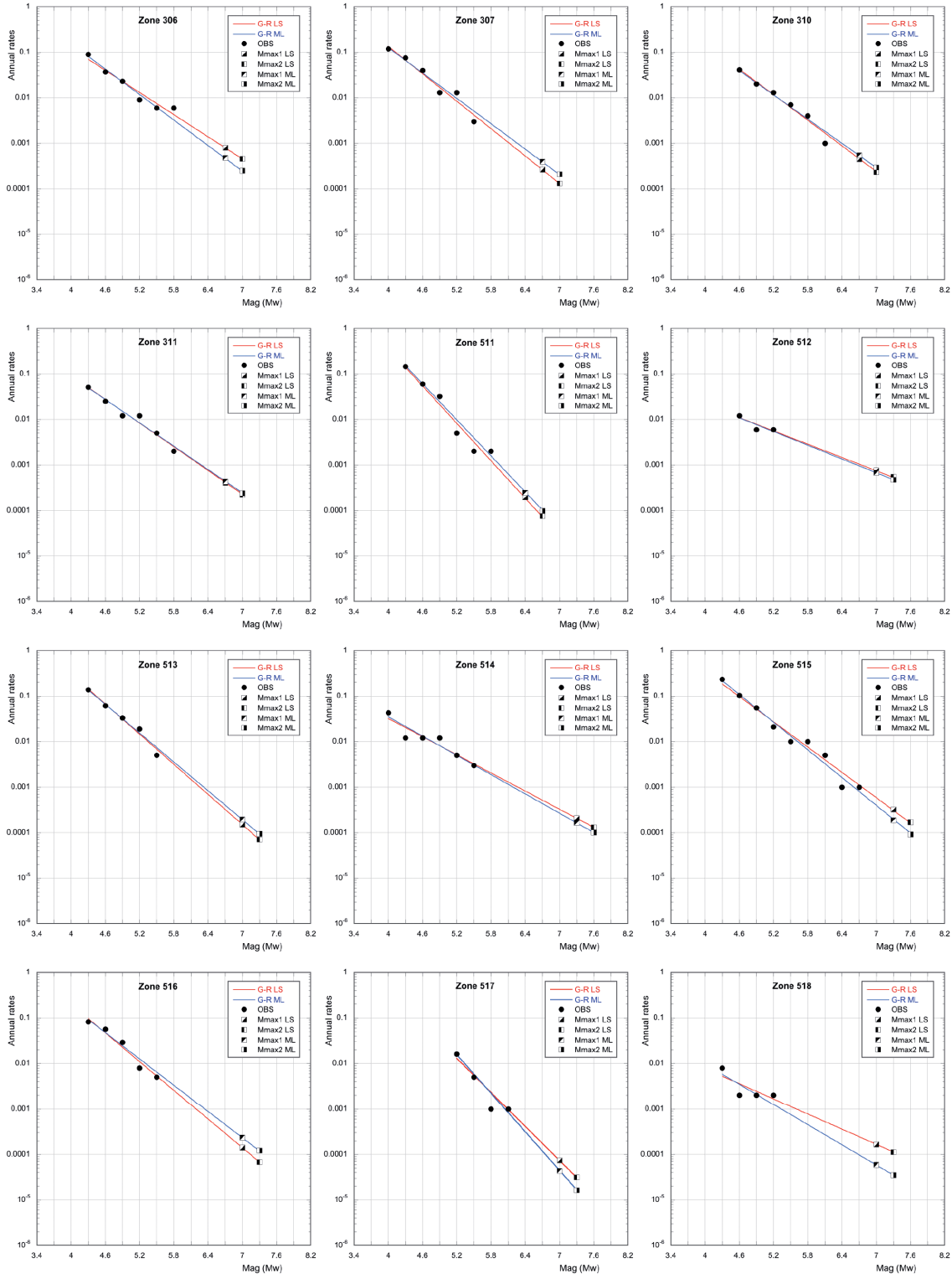

Fig. 7 - continued.

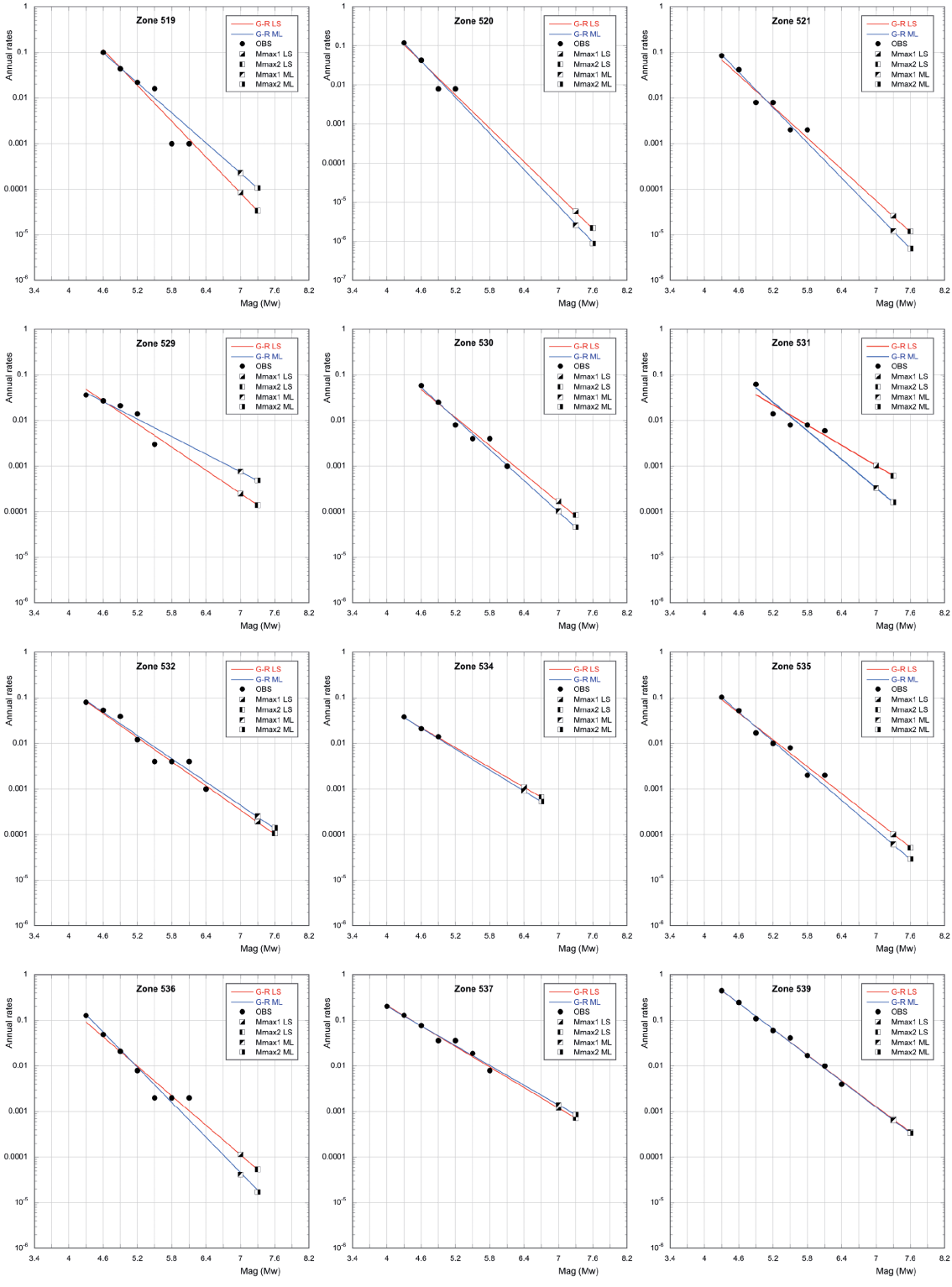

Fig. 7 - continued.

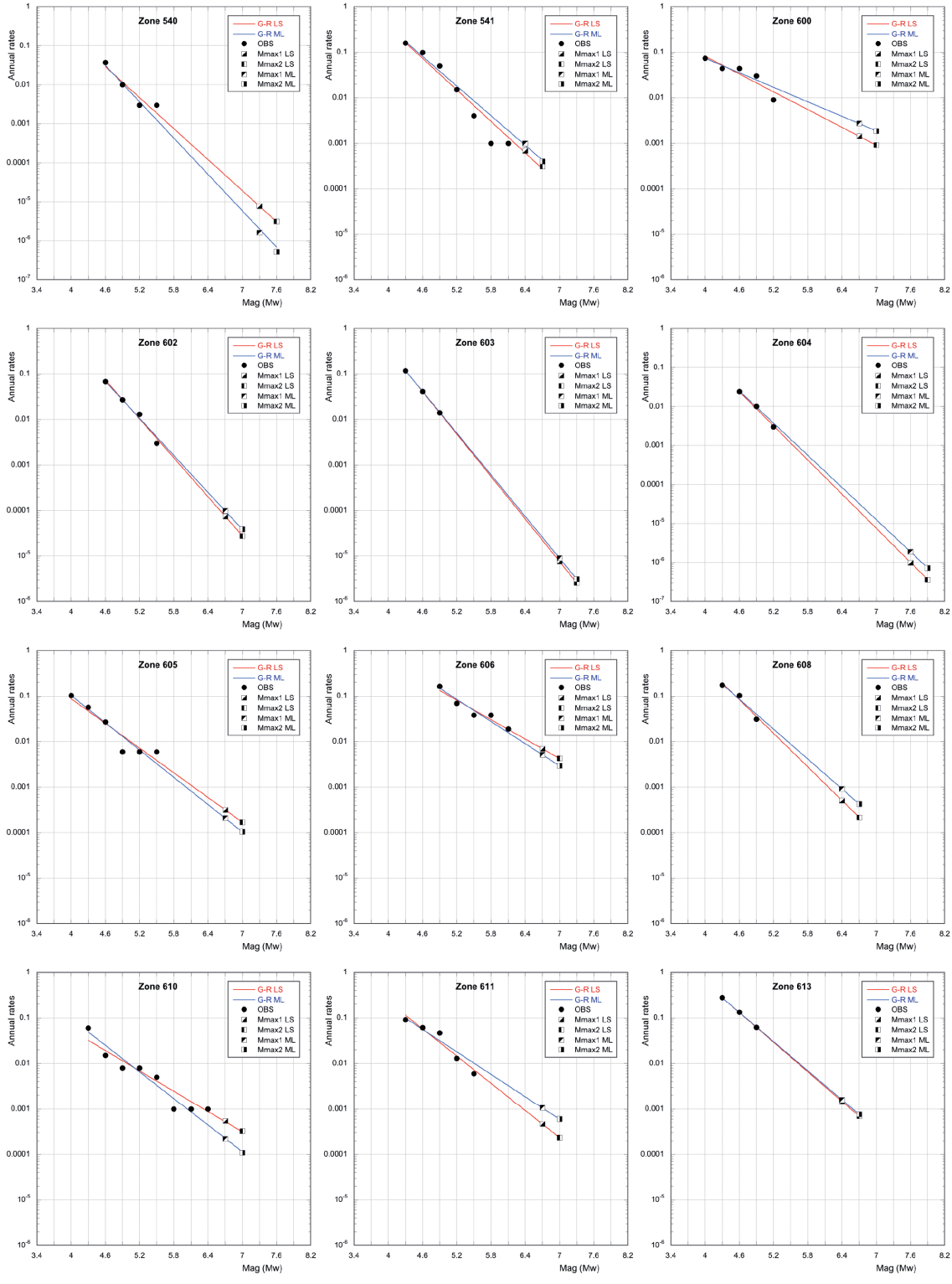

Fig. 7 - continued.

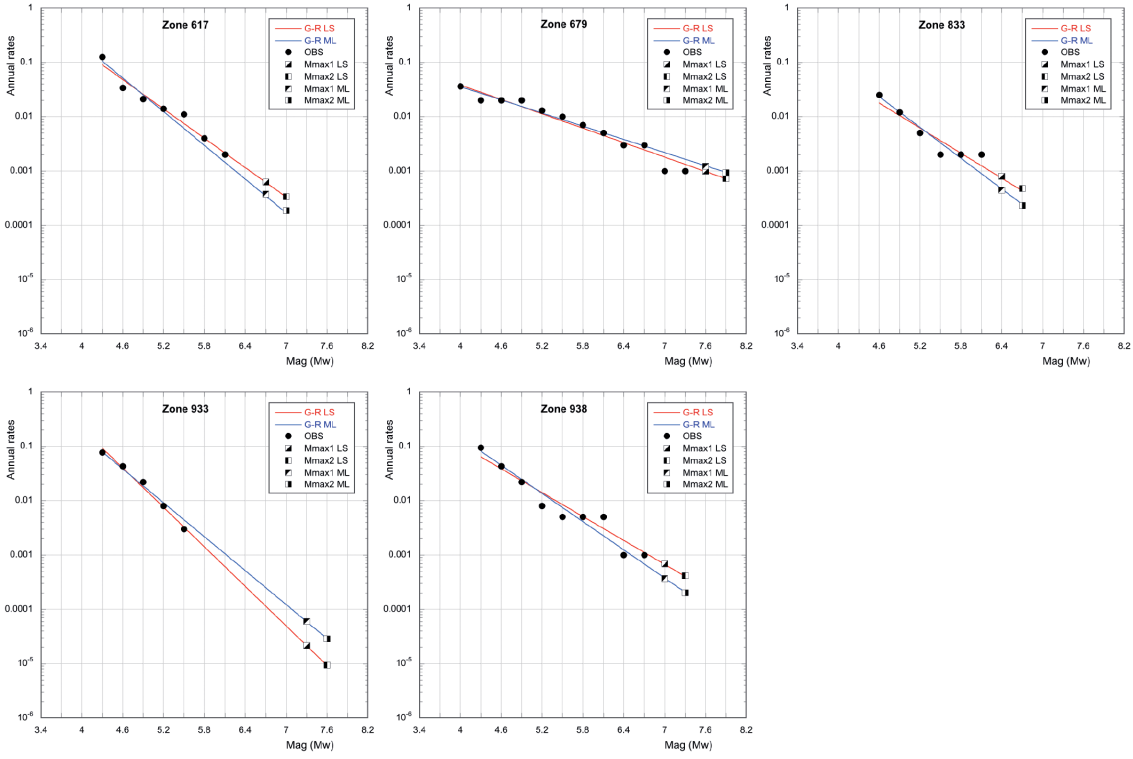

Fig. 7 - continued.

M_{max} was suggested by the general management of the MPS16 project and was evaluated for macro areas representing portions of the Italian territory and surroundings for which homogeneous tectonic behaviour is expected (Fig. 8). The data used for the M_{max} estimates have been taken from the CPTI15 earthquake catalogue (Rovida *et al.*, 2016) and the database of the composite seismogenic sources DISS 3.2.0 (DISS Working Group, 2015). Two values have been considered for M_{max}: M_{max1}, corresponding to the highest magnitude observed (in CPTI15), or computed from the dimensions (DISS 3.2.0) of the faults (Wells and Coppersmith, 1994), increased by its standard deviation; and M_{max2}, corresponding to M_{max1}+0.3. The correct duplets of M_{max} have been assigned to each SZ by a GIS overlay function with the related macro areas. The M_{max} rates have been computed by extrapolating the GR curves according to the two cited approaches (LS and ML). However, it is important to note that M_{max} bins with an annual rate smaller than 10^{-6} have not been considered in the hazard calculation.

Considering the small impact on hazard of M_{max} (see the following analyses) and, to a lesser extent, of the external SZs (because they are generally characterized by low seismicity), and the same type of magnitude considered by SHARE (Woessner *et al.*, 2015) and by the present study, the SHARE estimates for seismicity rates and M_{max} have also been directly adopted in the present study (Fig. 9 and Table 4). Actually, in the SHARE project, different approaches were adopted in low-to-moderate and in high seismicity regions (Woessner *et al.*, 2015) and for each SZ, four values of M_{max} were defined with decreasing weight values. In low-to-moderate seismicity regions (mainly those in the stable continental regions), a single distribution was assumed: the magnitude of the largest observed earthquake, with proper consideration of its uncertainty, was taken as the

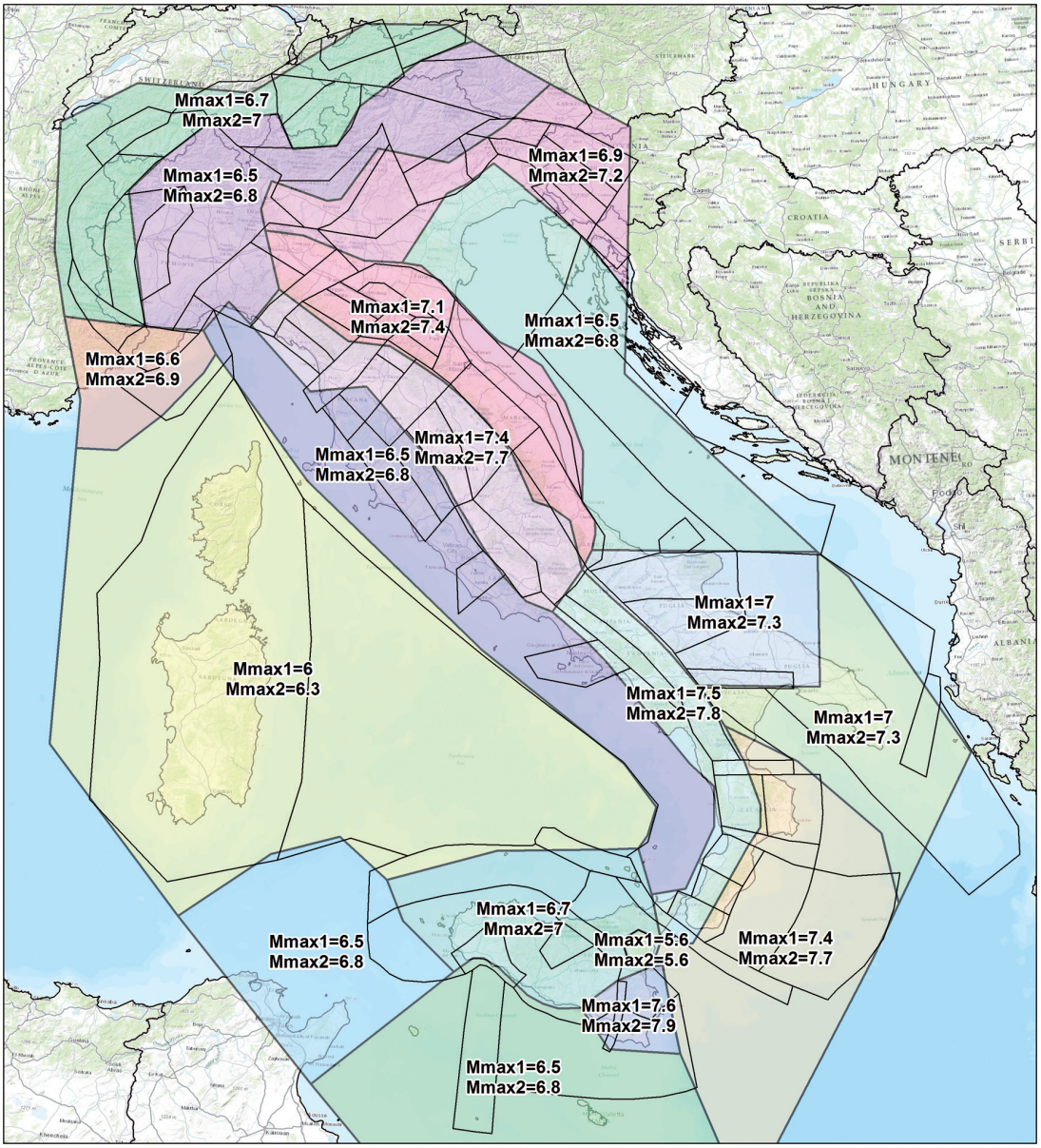

Fig. 8 - The A1 zonation (boxes with black perimeter) and macro areas (coloured polygons) identifying regions where M_{max} can be considered homogeneous.

lower value for the distribution of M_{max}, i.e., Mw = 6.5, whereas the other values were obtained by 0.2 increments (i.e., 6.7, 6.9, 7.1). In the remaining SZs, normally characterised by a high seismicity level and by a better knowledge of the historical seismicity and characterization of the seismogenic sources, the distribution of M_{max} was anchored to the larger value between the largest earthquake reported in the catalogue and the maximum magnitude expected according to the fault dimensions, again with consideration of its uncertainty; the other three larger M_{max} values were obtained by subsequent 0.2 increments. Also in this case, M_{max} bins with an annual rate smaller than 10^{-6} have not been considered in the hazard calculation.

Table 3 - GR parameters (*a*- and *b*-values) obtained by the LS and the ML approaches (for aLS, bLS, and aML, bML, respectively, see also GR-LS red line and GR-ML blue line, respectively, in Fig. 7) and M_{max1} and M_{max2} values, for each SZ of the A1 zonation.

No.	Mmin	aML	bML	aLS	bLS	M_{max1}	M_{max2}	N.Eq
101	4.3	3.280	0.96	5.310	1.410	6.9	7.2	22
102	4.6	4.690	1.25	3.220	0.980	6.9	7.2	26
103	4	1.920	0.72	3.080	0.980	6.9	7.2	17
106	4.3	5.040	1.38	4.490	1.270	6.9	7.2	19
107	4.3	5.730	1.51	4.940	1.340	6.9	7.2	27
108	4.3	0.670	0.57	0.090	0.460	6.9	7.2	5
109	4.3	1.750	0.83	0.710	0.620	6.9	7.2	3
110	4.3	5.820	1.47	5.800	1.480	6.9	7.2	44
112	4.3	3.020	0.95	2.510	0.850	6.9	7.2	18
113	4.6	2.510	0.86	1.440	0.660	6.9	7.2	13
114	4.3	2.930	0.89	3.020	0.900	6.9	7.2	33
200	4.3	2.430	0.680	2.180	0.630	7.5	7.8	64
201	4	2.700	1.020	1.980	0.850	6.5	6.8	5
202	4.6	5.390	1.410	6.080	1.560	7.5	7.8	16
203	4.6	2.110	0.760	1.460	0.640	7.5	7.8	12
204	4.9	4.240	1.180	2.950	0.950	7.5	7.8	11
205	4	2.180	0.710	2.260	0.730	7.5	7.8	26
206	4.6	3.670	1.130	0.380	0.400	7.1	7.4	12
207	4.6	5.402	1.360	3.976	1.050	7.1	7.4	2
208	4.3	2.290	0.770	2.290	0.770	7.5	7.8	15
212	4.6	5.353	1.360	3.887	1.050	7.1	7.4	4
213	4.3	1.740	0.780	0.790	0.590	7.5	7.8	3
214	4	0.900	0.620	0.580	0.560	7.1	7.4	2
215	4	1.810	0.700	2.420	0.840	7.0	7.3	11
216	4.3	1.150	0.560	0.790	0.490	7.0	7.3	10
217	4.3	3.130	0.850	3.460	0.920	7.0	7.3	45
219	4.3	0.460	0.490	0.460	0.490	7.5	7.8	6
221	4.3	4.560	1.350	4.830	1.410	6.5	6.8	8
224	4.3	3.300	0.98	4.680	1.280	6.5	6.8	18
225	4.3	3.780	0.92	3.650	0.890	7.4	7.7	125
226	4.3	3.610	1.03	2.410	0.800	7.1	7.4	31
301	4.6	2.810	0.97	1.000	0.630	6.6	6.9	10
302	4.3	5.180	1.53	5.180	1.530	6.5	6.8	5
303	4.3	2.690	0.91	2.320	0.840	6.6	6.9	9
304	4.3	2.910	0.93	2.330	0.810	6.7	7.0	14
305	4.6	4.900	1.43	5.452	1.550	6.5	6.8	5
306	4.3	5.407	1.4	5.860	1.500	6.7	7.0	37
307	4	2.760	0.92	3.190	1.010	6.7	7.0	17
310	4.6	2.700	0.89	2.950	0.940	6.7	7.0	11

Table 3 - continued.

No.	Mmin	aML	bML	aLS	bLS	M_{max1}	M_{max2}	N.Eq
311	4.3	2.330	0.85	2.370	0.860	6.7	7.0	9
511	4.3	4.900	1.33	5.060	1.370	6.5	6.8	22
512	4.6	0.400	0.51	0.170	0.470	7.1	7.4	5
513	4.3	3.640	1.05	3.880	1.100	7.1	7.4	24
514	4	1.400	0.71	1.210	0.670	7.4	7.7	5
515	4.3	3.790	1.03	3.300	0.930	7.4	7.7	38
516	4.3	3.020	0.95	3.570	1.060	7.1	7.4	15
517	5.2	5.580	1.42	4.620	1.250	7.1	7.4	14
518	4.3	1.020	0.75	0.140	0.560	7.1	7.4	2
519	4.6	4.130	1.11	5.170	1.320	7.1	7.4	29
520	4.3	5.730	1.55	5.060	1.410	7.4	7.7	18
521	4.3	4.430	1.28	3.740	1.140	7.4	7.7	16
529	4.3	1.290	0.63	2.350	0.850	7.1	7.4	8
530	4.6	4.060	1.15	3.370	1.020	7.1	7.4	19
531	4.9	3.800	1.04	2.190	0.740	7.1	7.4	20
532	4.3	2.610	0.85	2.640	0.870	7.4	7.7	14
534	4.3	1.820	0.76	1.710	0.730	6.5	6.8	5
535	4.3	3.600	1.07	3.160	0.980	7.4	7.7	17
536	4.3	4.580	1.28	3.620	1.080	7.1	7.4	22
537	4	2.190	0.72	2.260	0.740	7.1	7.4	31
539	4.3	3.670	0.94	3.690	0.940	7.4	7.7	78
540	4.6	5.960	1.61	4.530	1.320	7.4	7.7	9
541	4.3	3.970	1.1	4.130	1.140	6.5	6.8	27
600	4	1.050	0.540	1.510	0.650	6.7	7.0	10
602	4.6	4.970	1.340	5.450	1.430	6.7	7.0	14
603	4.3	5.660	1.530	5.730	1.550	7.1	7.4	15
604	4.6	4.760	1.380	5.090	1.460	7.6	7.9	4
605	4	3.020	1.000	2.600	0.910	6.7	7.0	10
606	4.9	3.070	0.800	2.600	0.710	6.7	7.0	8
608	4.3	4.000	1.100	4.640	1.240	6.5	6.8	6
610	4.3	2.970	0.990	1.760	0.750	6.7	7.0	8
611	4.3	2.520	0.820	3.370	1.000	6.7	7.0	14
613	4.3	4.050	1.070	4.080	1.080	6.5	6.8	6
617	4.3	3.480	1.030	2.760	0.890	6.7	7.0	14
679	4	0.340	0.440	0.340	0.440	7.6	7.9	8
833	4.6	2.730	0.95	1.770	0.760	6.5	6.8	8
933	4.3	3.440	1.05	4.170	1.210	7.4	7.7	13
938	4.3	2.730	0.88	1.950	0.730	7.1	7.4	15

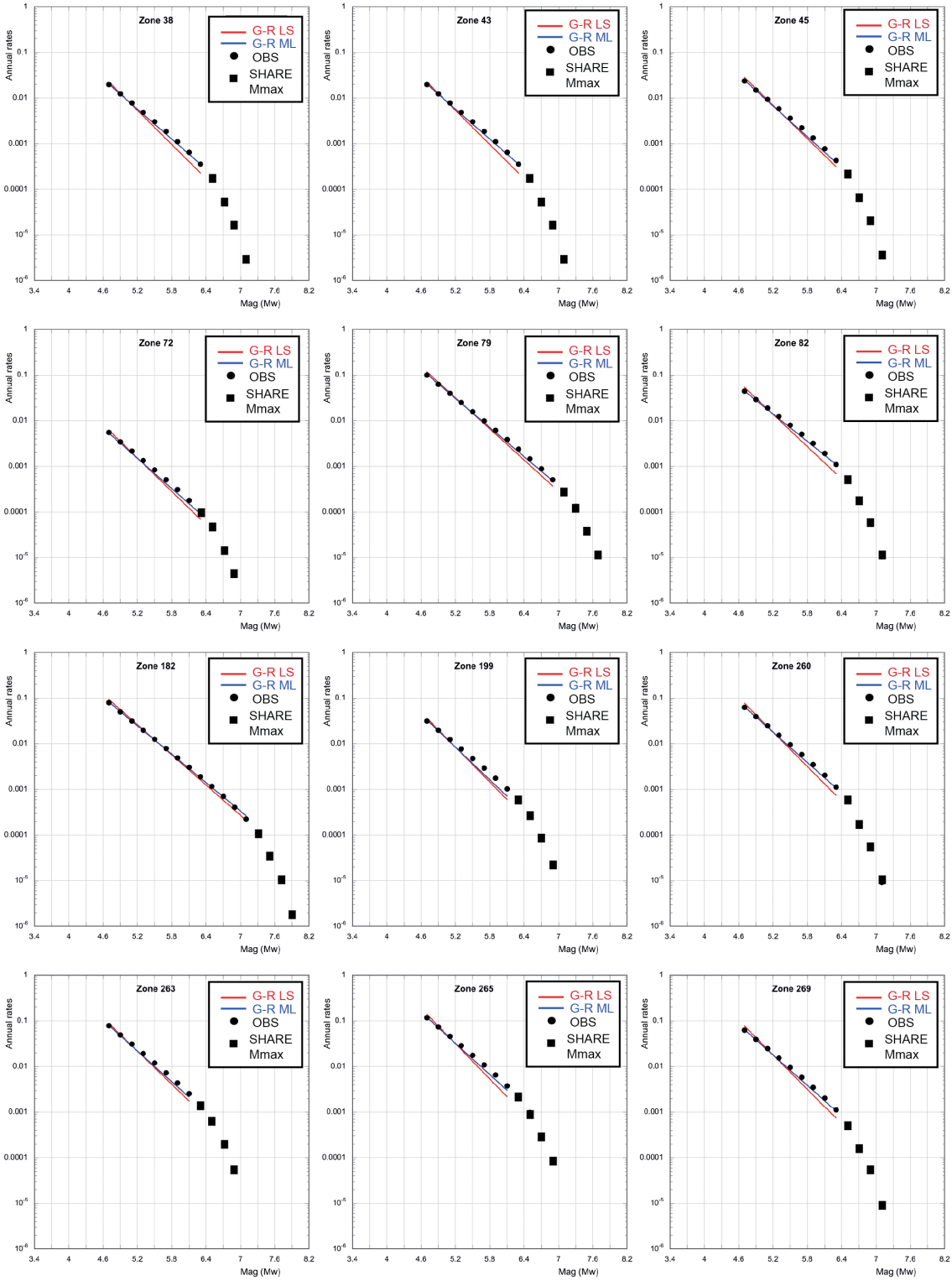

Fig. 9 - GR curves referring to the SHARE zonation, obtained by the Least Squares (red line, GR-LS) and the Maximum Likelihood (blue line, GR-ML) approaches. Black dots represent the observed individual seismicity rates. The four M_{max} values have been taken from the SHARE project (Woessner *et al.*, 2015).

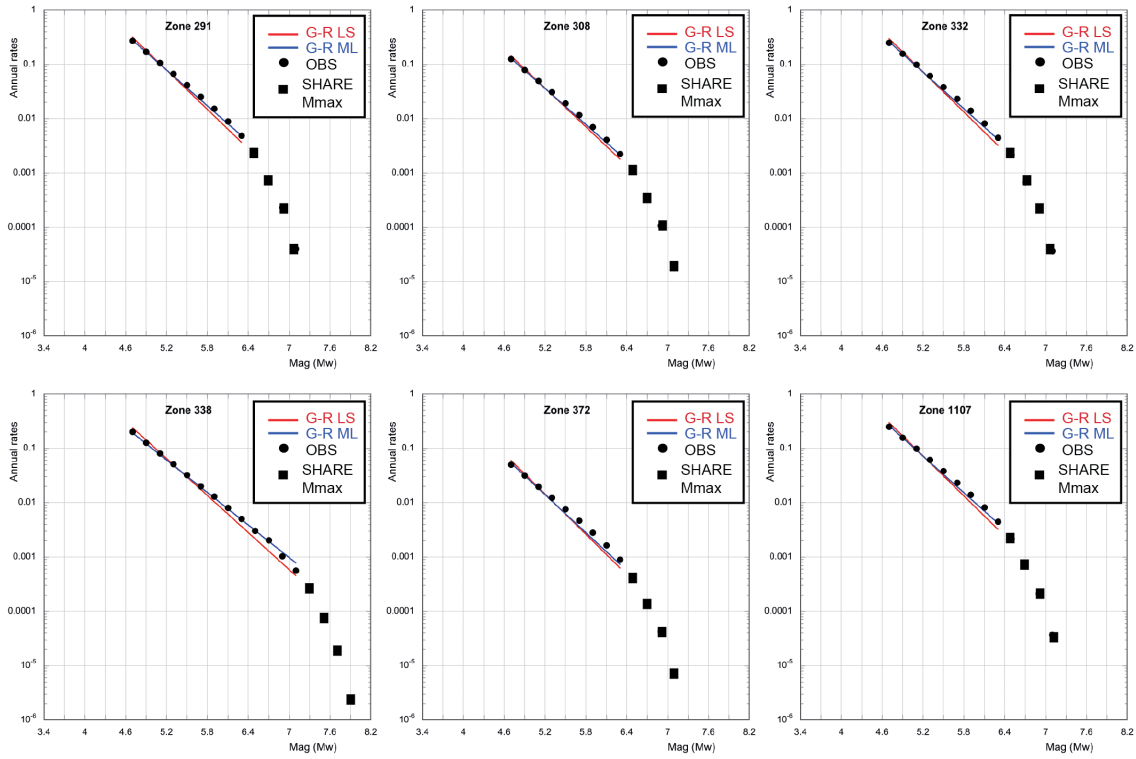

Fig. 9 - continued.

4. Results

As the suite of GMPEs to be applied for MPS16 have not been yet identified, in this preliminary seismic hazard assessment the Akkar *et al*. (2014) GMPE has been applied (see the branch AKK14 in Fig. 2), considering the Joyner-Boore distance. Fig. 10 shows the results, in terms of PGA with a 475-year return period, obtained for the six different branches: it can be seen that the differences introduced by the two values of M_{max} are marginal, while the three choices of seismicity rates lead to quite different hazard estimates. This aspect is well evident along the Apennines, where the northern, central, or both sectors show large expected PGA according to the different rate selection. It is surprising that the southern Apennines remain characterized by a lower hazard than the remaining parts of the chain, with the exception of the southernmost area in the case of the individual rate option (Figs. 10a and 10d). The final result of the elaboration is given by the weighted mean PGA value of the six branches (Fig. 11a): the northern Apennines and the eastern Alps appear as the most hazardous areas of Italy with values between 0.35 and 0.40 g. Almost all the rest of the Apennines is characterized by a PGA of between 0.275 and 0.30 g.

Cramer *et al*. (2002) have proposed the coefficient of variation (*COV*) in order to quantify the overall uncertainty of the results (see also Slejko *et al*., 2014), which is the standard deviation (σ) of the estimated *PGA* variation at each point divided by the mean value at that point ($COV = \sigma / PGA_{mean}$). It can be seen from Fig. 12a that the *COV* value computed for the estimates presented here remains below 20% everywhere but the western Alps. This means that there is not a large uncertainty associated with the hazard estimates introduced by the logic tree. It is clear that a logic

Table 4 - GR parameters (*a*- and *b*-values) for each SHARE SZs. aML, bML, M_{max}, and WM indicate, respectively, the GR parameters calculated with the ML method, the M_{max} values and their weights, calculated in the frame of the SHARE project. aLS and bLS indicate the GR parameters calculated with the LS method in the present study on the basis of the SHARE individual seismicity rates.

No.	M_{min}	aML	bML	aLS	bLS	M_{max1}	M_{max2}	M_{max3}	M_{max4}	WM1	WM2	WM3	WM4
38	4.7	3.45	1.1	4.08	1.22	6.6	6.8	7.0	7.2	0.5	0.2	0.2	0.1
43	4.7	3.45	1.1	4.08	1.22	6.6	6.8	7.0	7.2	0.5	0.2	0.2	0.1
45	4.7	3.53	1.1	4.16	1.22	6.6	6.8	7.0	7.2	0.5	0.2	0.2	0.1
72	4.7	2.9	1.1	3.53	1.22	6.6	6.8	7.0	7.2	0.5	0.2	0.2	0.1
79	4.7	3.88	1.04	4.43	1.14	7.3	7.5	7.7	7.9	0.5	0.2	0.2	0.1
82	4.7	3.43	1.02	4.06	1.14	6.6	6.8	7.0	7.2	0.5	0.2	0.2	0.1
182	4.7	3.73	1.03	4.25	1.12	7.3	7.5	7.7	7.9	0.5	0.2	0.2	0.1
199	4.7	3.81	1.13	4.46	1.26	6.5	6.7	6.9	7.1	0.5	0.2	0.2	0.1
260	4.7	3.95	1.1	4.58	1.22	6.6	6.8	7.0	7.2	0.5	0.2	0.2	0.1
263	4.7	4.21	1.13	4.86	1.26	6.5	6.7	6.9	7.1	0.5	0.2	0.2	0.1
265	4.7	4.38	1.13	5.03	1.26	6.5	6.7	6.9	7.1	0.5	0.2	0.2	0.1
269	4.7	3.95	1.1	4.58	1.22	6.6	6.8	7.0	7.2	0.5	0.2	0.2	0.1
291	4.7	4.59	1.1	5.22	1.22	6.6	6.8	7.0	7.2	0.5	0.2	0.2	0.1
308	4.7	4.25	1.1	4.88	1.22	6.6	6.8	7.0	7.2	0.5	0.2	0.2	0.1
332	4.7	4.55	1.1	5.18	1.22	6.6	6.8	7.0	7.2	0.5	0.2	0.2	0.1
338	4.7	4.14	1.03	4.65	1.12	7.4	7.6	7.8	8.0	0.5	0.2	0.2	0.1
372	4.7	3.85	1	4.48	1.22	6.6	6.8	7.0	7.2	0.5	0.2	0.2	0.1
1107	4.7	4.55	1.1	5.18	1.29	6.6	6.8	7.0	7.2	0.5	0.2	0.2	0.1

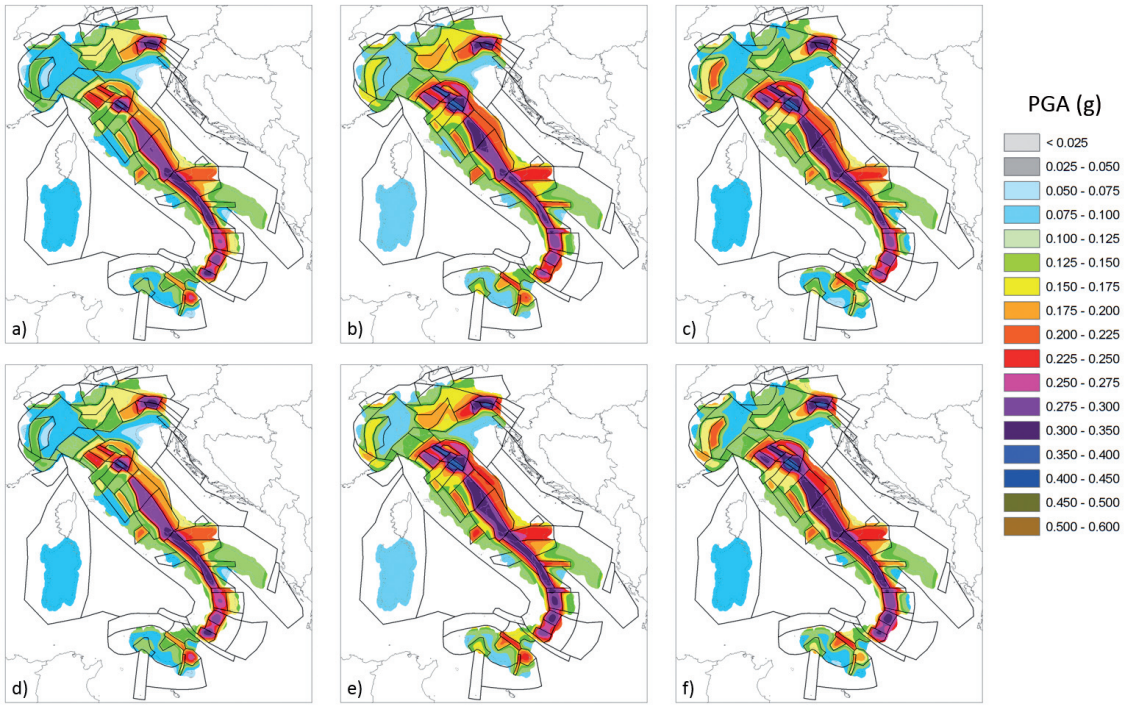

Fig. 10 - PGA with a 475-year return period obtained from the six branches of the logic tree, A1 zonation and the AKK14 GMPE with Joyner-Boore distance: a) M_{max1} and IR; b) M_{max1} and GR-ML; c) M_{max1} and GR-LS; d) M_{max2} and IR; e) M_{max2} and GR-ML; f) M_{max2} and GR-LS.

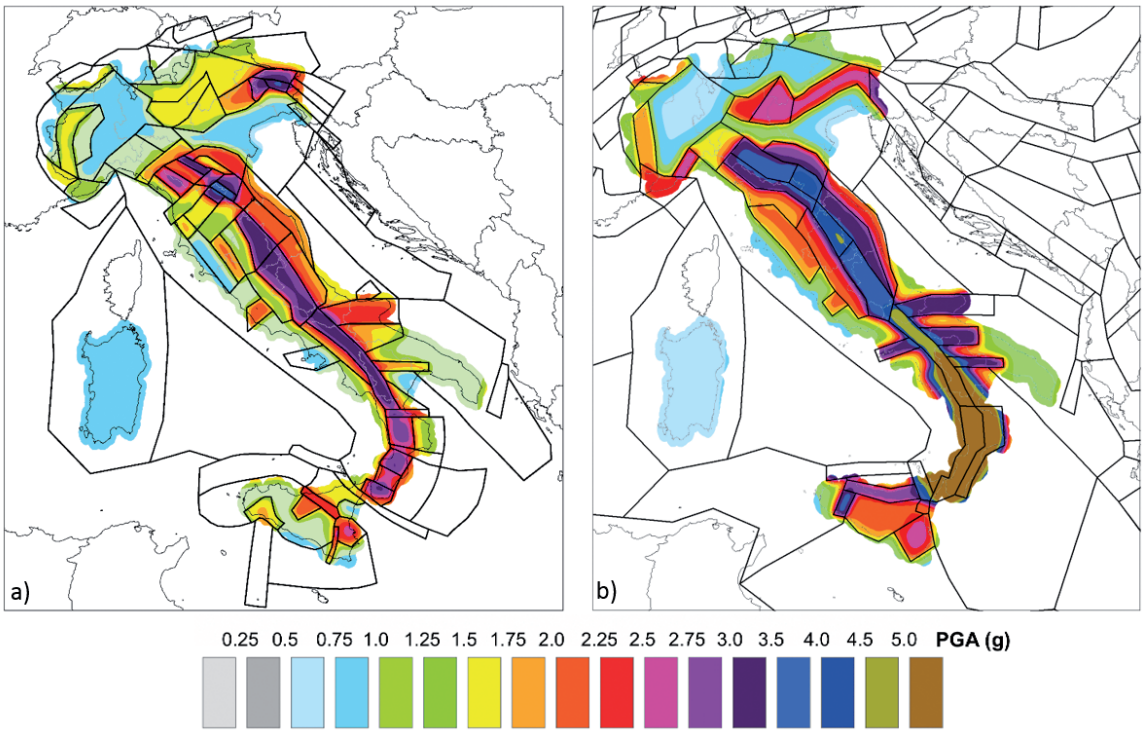

Fig. 11 - PGA with a 475-year return period calculated by the AKK14 GMPE with Joyner-Boore distance: a) A1 zonation (weighted mean of the six branches of the logic tree, see Fig. 10); b) re-elaborated SHARE map (see the text for details).

tree with a larger number of branches, i.e., with more options for the input parameters, would have implied a larger epistemic uncertainty on the mean results, but the hazard computation shown here simply represents the impact of the new zonation.

The influence of the individual input parameters in the final hazard results is smoothed by the use of several different hypotheses (branches). To explore this aspect, i.e., to determine individual branch-point sensitivity, we have computed the individual coefficient of variation (*ICOV*) for each alternative (node) of the logic tree (seismicity models and M_{max}). Each *ICOV* map represents the relative contribution of the uncertainty in that variable to the overall uncertainty presented in the *COV* map, while all the other variables remain fixed. As no sensible difference is obtained using one or the other branches of the fixed variable, the branches related to M_{max1} have been considered in the computation of the *ICOV* of seismicity rate (Fig. 12b) and those referring to GR-ML for *ICOV* of M_{max} (Fig. 12c). It can be seen that the major contribution to the overall uncertainty comes from the seismicity models (Fig. 12b), while M_{max} has almost no influence for the 475-year return period (Fig. 12c). In fact, the *ICOV* map for the seismicity models (Fig. 12b) shows only marginal differences with respect to the *COV* map (Fig. 12a).

The first step in evaluating the quality of the calculated hazard map consists of a comparison between the number of events contained in the earthquake catalogue and those used in the hazard computation. More precisely, the completeness periods of the Apennines (Centre in Fig. 4) have been considered suitable for all of Italy, because it refers the largest and best documented macro area and the related number of quakes in the CPTI15 catalogue has been computed and

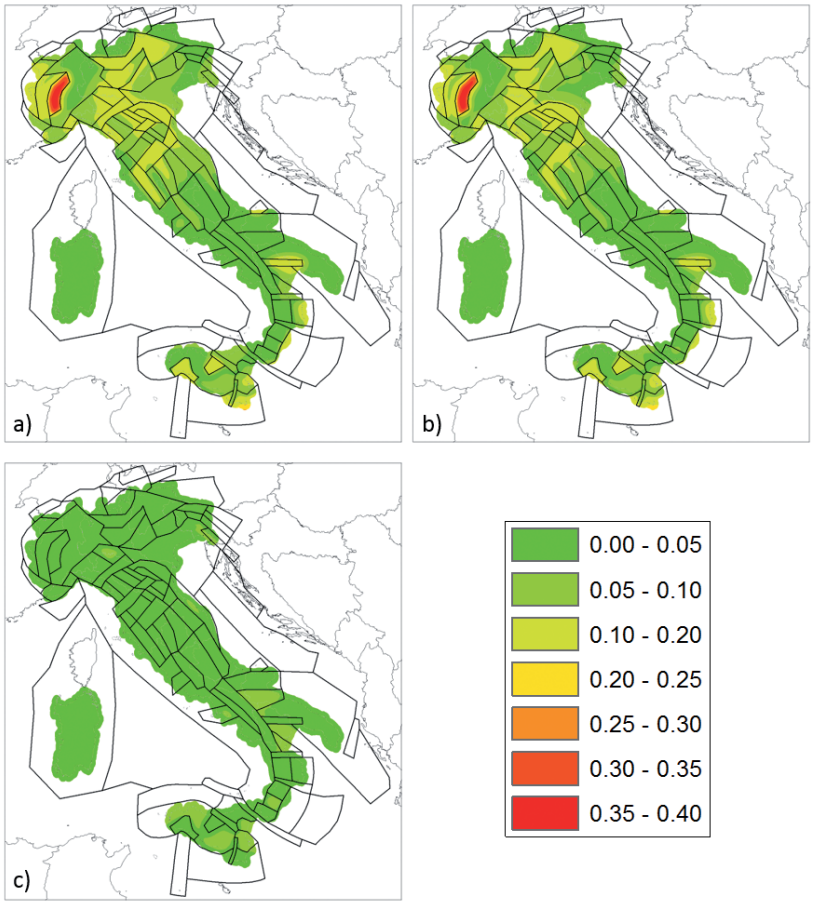

Fig. 12 - Representation of the epistemic uncertainty introduced by the logic tree: a) *COV*; b) *ICOV* for the node of the seismicity rates; c) ICOV for the node of M_{max}. As the number of branches considered is limited, almost all epistemic uncertainty relates to the different choices of the seismicity rates.

normalized to one year. These rates have been compared with the sum of those obtained after the ML interpolation and used as input for the different SZs (Fig. 13). It can be seen that only for a M_W larger than, or equal to, 7 (very rare extreme values with an annual frequency of 0.02 and lower), the observed rates are larger than those used in the present elaboration.

To investigate the differences introduced by the present seismogenic zonation with respect to the previous ones, a re-elaboration of the SHARE map has been performed. It is worth noting that, because the seismogenic information (in terms of zonation and associated seismicity rates) used as input for one of the source models considered for the SHARE map and that used for the MPS04 map are very similar (Meletti *et al.*, 2014), the comparison presented here holds for both SHARE and MPS04 maps. Entering into the details of the comparison presented here, the input of SHARE, in terms of seismogenic zones and related seismicity rates, has been used with the Akkar *et al.* (2014) GMPE (Fig. 11b). Comparing the A1 map (Fig. 11a) with the re-elaborated SHARE map (Fig. 11b), the higher PGA of this latter map is evident almost throughout the Italian territory. The difference is about 0.1 g, with the exception of the southern Apennines, where the difference is even larger, and the easternmost sector of the Alps, where, conversely, the A1 map shows a larger PGA.

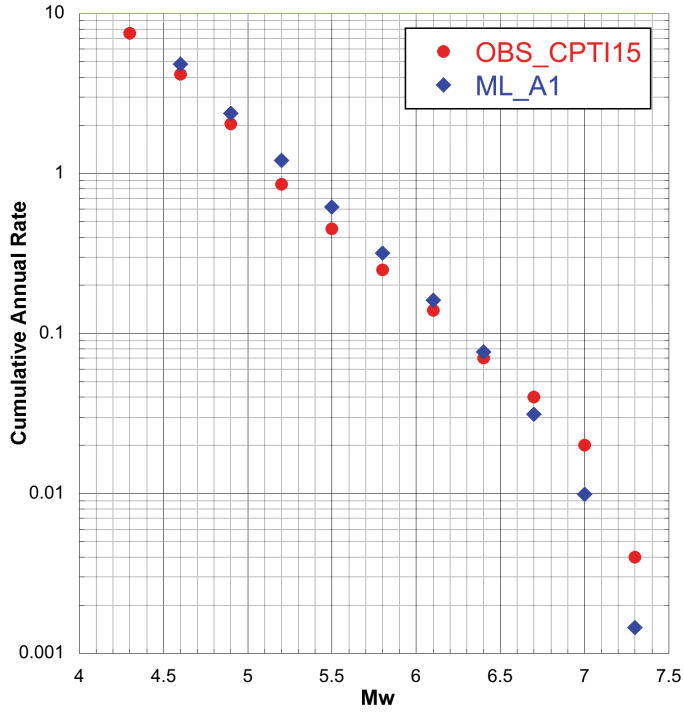

Fig. 13 - Observed seismicity rates from the CPTI15 catalogue (red dots), according to the completeness periods of the Apennines (Centre in Fig. 4), and sum of the computed seismicity rates (obtained by ML interpolation) for the different SZs (blue diamonds).

5. Conclusions

The A1 zonation presented here has been developed as one of the branches of the logic tree designed for the new Italian seismic hazard map MPS16. This new zonation is generally more detailed than the current national zonation ZS9 (Meletti *et al.*, 2008) and the principal new features of the A1 zonation are: 1) a subdivision of some large zones of the current national zonation ZS9 (Meletti *et al.*, 2008), which, in the authors' opinion, includes seismogenic structures with different geometry and failure mechanisms; and 2) the introduction of new SZs not considered seismogenic until now. It is worth noticing that in some areas the difference between the newly constructed SZs and those of ZS9 has been deemed negligible, in terms of geographical boundaries and seismotectonic characteristics.

The new version of the Italian Parametric Catalogue CPTI15 (Rovida *et al.*, 2016) has been used for the seismicity rate definition, and, to compute the preliminary hazard results, the Akkar *et al.* (2014) GMPE has been applied, using the Joyner-Boore distance. The comparison between the number of events contained in the CPT15 earthquake catalogue and those used in the hazard computation (Fig. 13) shows a good agreement, suggesting an acceptable representation of past seismicity in the present seismic characterization of the SZs. The obtained map (Fig. 11a) shows the maximum expected ground motion all along the Apennines and in the eastern Alps. Its comparison with a re-elaboration of the SHARE map (Fig. 11b), where a similar attenuation model has been applied, shows a general agreement in the identification of the most seismic areas, while the absolute values are rather different. In fact the SHARE map forecasts slightly stronger shaking.

It is worth noting that the hazard results are only preliminary and initiated by a global reviewing process in progress among all zonations expected to contribute to the future national seismic hazard map. The elaboration presented here, in fact, highlights rather well some weak points in the source characterization. For example, the seismicity of some SZs (Fig. 7) is poorly constrained by the available seismicity rates, leading to a debatable GR *b*-value. This failure needs to be fixed either with modifications on the SZ geometry or merging some similar SZs only for the *b*-value computation (see Schmid and Slejko, 2009).

In conclusion, while the seismogenic zonation seems well founded from the geological point of view, its seismic characterization needs improvement. The elaboration of seismic hazard presented here is the way to provide that improvement.

Acknowledgements. Many thanks are due to Dario Albarello and an anonymous reviewer for improving our manuscript.

REFERENCES

Aki K.; 1965: *Maximum likelihood estimate of b in the formula logN=a-bM and its confidence limits*. Bull. Earthquake Res. Inst., **43**, 237-239.

Akkar S., Sandikkaya M.A. and Bommer J.J.; 2014: *Empirical ground-motion models for point- and extended-source crustal earthquake scenarios in Europe and the Middle East*. Bull. Earthquake Eng., **12**, 359–387.

Barani S., Spallarossa D., Bazzurro P. and Eva C.; 2007: *Sensitivity analysis of seismic hazard for western Liguria (north western Italy): a first attempt towards the understanding and quantification of hazard uncertainty*. Tectonophysics, **435**, 1–4, 13-35. ISSN 0040-1951, http://dx.doi.org/10.1016/j.tecto.2007.02.008.

Barani S., Scafidi D. and Eva C.; 2010: *Strain rates in northwestern Italy from spatially smoothed seismicity*. J. Geophys. Res, **115**, B07302, doi:10.1029/2009JB006637.

Coppersmith K.J. and Youngs R.R.; 1986: *Capturing uncertainty in probabilistic seismic hazard assessments within intraplate environments*. In: Proceedings of the Third U.S. National Conference on Earthquake Engineering, August 24-28, 1986, Charleston, SC, Earthquake Engineering Research Institute, El Cerrito CA U.S.A., **1**, pp. 301-312.

Cornell C.A.; 1968: *Engineering seismic risk analysis*. Bull. Seism Soc. Am., **58**, 1583-1606.

Cramer C.H., Wheeler R.L. and Mueller C.S.; 2002: *Uncertainty analysis for seismic hazard in the southern Illinois basin*. Seism. Res. Lett., **73**, 792-805.

Delacou B., Sue C., Nocquet J.M., Champagnac J.D., Allanic C. and Burkhard M.; 2008: *Quantification of strain rate in the western Alps using geodesy-comparison with seismotectonics*. Swiss J. Geosci., **101**, 377-385, doi:10.1007/s00015-008-1271-3.

DISS Working Group; 2015: *Database of individual seismogenic sources (DISS), Version 3.2.0: A compilation of potential sources for earthquakes larger than M 5.5 in Italy and surrounding areas*. http://diss.rm.ingv.it/diss/, © INGV 2015 - Istituto Nazionale di Geofisica e Vulcanologia. DOI:10.6092/INGV.IT-DISS3.2.0.

Gardner J.K. and Knopoff L.; 1974: *Is the sequence of earthquakes in southern California, with aftershocks removed, Poissonian?* Bull. Seism. Soc. Am., **64**,1363–1367.

Gasperini P., Bernardini F., Valensise G. and Boschi E.; 1999: *Defining seismogenic sources from historical earthquake felt reports*. Bull. Seism. Soc. Am., **89**, 94-110.

ISIDe Working Group; 2015: *Database of seismic events of Italy (1981-present)*. <http://iside.rm.ingv.it>.

Kulkarni R.B., Youngs R.R. and Coppersmith K.J.; 1984: *Assessment of confidence intervals for results of seismic hazard analysis*. In: Proceedings of the Eighth World Conference on Earthquake Engineering, July 21-28, 1984, San Francisco CA U.S.A., Prentice-Hall Inc., Englewood Cliffs NJ U.S.A., **1**, 263-270.

Martelli L., Bonini M., Calabrese L., Corti G., Ercolessi G., Molinari F.C., Piccardi L., Pondrelli S., Sani F. and Severi P.; 2017a: *Note illustrative della carta sismotettonica della Regione Emilia Romagna ed aree limitrofe*. Dream, 93 pp.

Martelli L., Ercolessi G., Sani F., Bonini M., Corti G., Santulin M., Tamaro A., Rebez A. and Slejko D.; 2017b: *Analisi 3D della pericolosità sismica dell'Appennino settentrionale. Proposta di nuova zonazione sismogenica e analisi della pericolosità sulla base di un modello 3D delle sorgenti sismiche*. Centro Stampa Regione Emilia-Romagna, Bologna, 36 pp.

Martelli L., Santulin M., Sani F., Tamaro A., Bonini M., Rebez A., Corti G. and Slejko D.; 2017c: *Seismic hazard of the Northern Apennines based on 3D seismic sources*. J Seismol., doi: 10.1007/s10950-017-9665-1.

McGuire R.K.; 1977: *Seismic design spectra and mapping procedures using hazard analysis based directly on oscillator response*. Earthq. Engin. Struct. Dyn., **5**, 211-234.

McGuire R.K. and Shedlock K.M.; 1981: *Statistical uncertainties in seismic hazard evaluations in the United States*. Bull. Seism. Soc. Am., **71**, 1287-1308.

Meletti C., Patacca E. and Scandone P.; 2000: Construction of a seismotectonic model: the case of Italy. Pure Appl. Geophys., **157**, 11-35.

Meletti C., Galadini F., Valensise G., Stucchi M., Basili R., Barba S., Vannucci G. and Boschi E.; 2008: *A seismic source zone model for the seismic hazard assessment of the Italian territory.* Tectonophysics, **450**, 85–108.

Meletti C., Rovida A., D'Amico V. and Stucchi M.; 2014: *Modelli di pericolositá sismica per l'area italiana: "MPS04-S1" e "SHARE"*. Progettazione Sismica, **5**(1), 15-25, doi: 10.7414/PS.5.1.15-25.

Ordinanza PCM 3274; 2003: *Primi elementi in materia di criteri generali per la classificazione del territorio nazionale e di normative tecniche*. Gazzetta Ufficiale n.105 del 08/05/2003, <http://zonesismiche.mi.ingv.it/documenti/gazzetta.pdf>.

Pagani M., Monelli D., Weatherill G., Danciu L., Crowley H., Silva V., Henshaw P., Butler L., Nastasi M., Panzeri L., Simionato and M., Vigano D.; 2014: *OpenQuake-engine: an open hazard (and risk) software for the global earthquake model*. Seismol. Res. Lett., **85**, 692-702.

Pondrelli S., Salimbeni S., Morelli A., Ekström G., Postpischl L., Vannucci G. and Boschi E.; 2011: *European-mediterranean regional centroid moment tensor catalog: solutions for 2005-2008*. Phys Earth Planet Int 185. doi: 10.1016/j.pepi.2011.01.007.

Rebez A. and Slejko D.; 2000: *Sensitivity analysis on the input parameters in probabilistic seismic hazard assessment*. Soil Dynamics and Earthquake Engineering, **20,** 341-351.

Rovida A., Camassi R., Gasperini P. and Stucchi M. (a cura di); 2011: *CPTI11, la versione 2011 del Catalogo Parametrico dei Terremoti Italiani*. Milano, Bologna, http://emidius.mi.ingv.it/CPTI.

Rovida A., Locati M., Camassi R., Lolli B. and Gasperini P.; 2016: *CPTI15, the 2015 version of the parametric catalogue of italian earthquakes*. *Istituto Nazionale di Geofisica e Vulcanologia*. doi:http://doi.org/10.6092/INGV.IT-CPTI15.

Scafidi D., Barani S., De Ferrari R., Ferretti G., Pasta M., Pavan M., Spallarossa D. and Turino C.; 2015: *Seismicity of northwestern Italy during the last thirty years*. Journal of Seismology, **19**, 201-218.

Schmid S.M. and Slejko D.; 2009: *Seismic source characterization of the Alpine foreland in the context of a probabilistic seismic hazard analysis by PEGASOS Expert Group 1 (EG1a)*. Swiss J. Geosci., **102**, 121-148, doi: 10.1007/s00015-008-1300-2.

Slejko D., Peruzza L. and Rebez A.; 1998: *Seismic hazard maps of Italy*. Annali di Geofisica, **41**, 183-214.

Slejko D., Carulli G.B., Riuscetti M., Cucchi F., Grimaz S., Rebez A., Accaino F., Affatato A., Biolchi S., Nieto D., Puntel E., Sanò T., Santulin M., Tinivella U. and Zini L.; 2011: Soil characterization and seismic hazard maps for the Friuli Venezia Giulia region (NE Italy). Boll. Geof. Teor. Appl., **52**, 59-104.

Slejko D., Santulin M. and Garcia J.; 2014: *Seismic hazard estimates for the area of Pylos and surrounding region (SW Peloponnese) for seismic and tsunami risk assessment*. Boll. Geof. Teor. Appl., **55**, 433-468. doi:10.4430/bgta0090.

Stucchi M., Meletti C., Montaldo V., Crowley H., Calvi G.M. and Boschi E.; 2011: *Seismic hazard assessment (2003–2009) for the Italian building code*. Bull. Seism. Soc. Am., **101**, 1885–1911. doi: 10.1785/0120100130.

Toro G.R., Abrahamson N.A. and Schneider J.F.; 1997: *Model of strong motions from earthquakes in central and eastern North America: best estimates and uncertainties*. Seism. Res. Lett., **68**, 41-57.

Utsu T.; 1965: *A method for determining the value of b in the formula logN=a-bM showing the magnitude-frequency relation for earthquakes*. Geophys. Bull. Hokkaido Univ., **13**, 99-103.

Utsu T.; 1966: *A statistical significance test of the difference in b-value between two earthquake groups*. J. Phys. Earth, **14**, 37-40.

Weichert D.H.; 1980: *Estimation of the earthquake recurrence parameters for unequal observation periods for different magnitudes*. Bull. Seismol. Soc. Am., **70**, 1337-1346.

Wells D.L. and Coppersmith K.J.; 1994: *New empirical relationship among magnitude, rupture length, rupture width, rupture area, and surface displacement*. Bull. Seism. Soc. Am., **84**, 974-1002.

Woessner J., Danciu L., Giardini D., Crowley H., Cotton F., Grünthal G., Valensise G., Arvidsson R., Basili R., Demircioglu M.N., Hiemer S., Meletti C., Musson R.W., Rovida A.N., Sesetyan K., Stucchi M. and the SHARE consortium; 2015: *The 2013 European seismic hazard model: key components and results*. Bull. Earthq. Eng., **13**, 3553–3596, doi:10.1007/s10518-015-9795-1.

Corresponding author: Marco Santulin
Istituto Nazionale di Geofisica e Vulcanologia, sezione di Milano, c/o OGS, Trieste
Borgo Grotta Gigante 42c, 34010 Sgonico (TS), Italy
Phone: +39 040 2140299; e-mail: msantulin@inogs.it